Accepted Manuscript

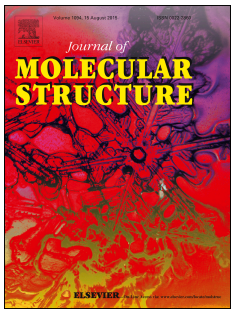

Synthesis, spectroscopic and electrochemical characterization of secnidazole esters

Hafiz Abdullah Shahid, Sajid Jahangir, Muddasir Hanif, Tianrou Xiong, Haji Muhammad, Sana Wahid, Sammer Yousuf, Naseem Qureshi

PII: S0022-2860(17)31104-3

DOI: 10.1016/j.molstruc.2017.08.036

Reference: MOLSTR 24174

To appear in: *Journal of Molecular Structure*

Received Date: 25 June 2017

Revised Date: 9 August 2017

Accepted Date: 10 August 2017

Please cite this article as: H.A. Shahid, S. Jahangir, M. Hanif, T. Xiong, H. Muhammad, S. Wahid, S. Yousuf, N. Qureshi, Synthesis, spectroscopic and electrochemical characterization of secnidazole esters, *Journal of Molecular Structure* (2017), doi: 10.1016/j.molstruc.2017.08.036.

Graphical Abstract:

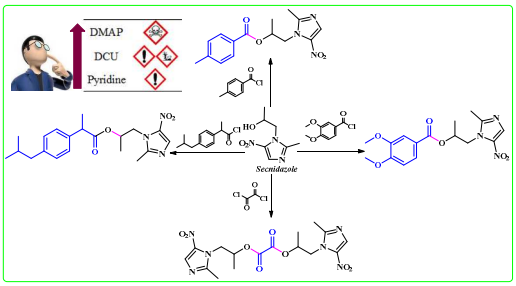

Synthesis, spectroscopic and electrochemical characterization of secnidazole esters

Hafiz Abdullah Shahid,[a] Sajid Jahangir,[a]* Muddasir Hanif,[b]* Tianrou Xiong [b],

Haji Muhammad,[a] Sana Wahid, Sammer Yousuf,[c] Naseem Qureshi,[d]*

[a]*Department of Chemistry, Faculty of Science, Federal Urdu University of Arts, Science and Technology, Gulshan-e-Iqbal, Karachi 75300, Pakistan*

[b]*Department of Chemistry and Chemical Engineering, Jiangxi Normal University, Nanchang, Jiangxi 330022, People's Republic of China*

[c]*HEJ Research Institute of Chemistry, International Center for Chemical and Biological Sciences, University of Karachi, Karachi 75270, Pakistan*

[d]*Department of Chemistry, Karakoram International University, Gilgit-Baltistan,15100 Gilgit, Pakistan*

*Corresponding Authors; E-mail: sajid.jahangir@fuuast.edu.pk (S. J.), muddasirhanif@yahoo.com (M. H.), ngq18@hotmail.com (N.Q.)

Abstract: We report a low-cost, less toxic to environment and simple method for the esterification of secnidazole. This is first comprehensive structural characterization of novel secnidazole esters by the spectroscopic and electrochemical methods. The important EIMS fragmentation analysis showed unique contribution of heteroatom bonds explained by the fragmentation patterns. These peaks originate from the loss of single electron, loss of HCN, M-O, M-NO, M-NO_2, M-$C_7H_{10}N_3O_3$, and M-$C_8H_{10}N_3O_4$. The comparison of ^{13}C NMR predicted values with the experimental values showed that ChemBioDraw Ultra 14.0 has advantage of predicting aromatic (sp^2) carbons, while MestReNova 6.1 predicts sp^3 hybrid carbons more accurately. The electrochemical properties indicated an irreversible oxidation process and reversible reduction process in these ester molecules similar to the parent secnidazole.

Keywords: Synthesis, EIMS fragmentation, Hetero Atom, Spectroscopic Characterization, NMR prediction, Electrochemistry

1. Introduction

Esterification is a well-known and very important reaction in chemistry. The German chemist Leopold Gmelin (1788-1853) born in Göttingen into a distinguished family of chemists, coined the word “ester”. [1] Esters are widespread in nature (eg. triesters) [2-4] found in many types of food and responsible for the characteristic aroma and medicinal effects.[5-8] Polyesters, polyethylene terephthalate, acrylate esters, and cellulose acetate are some examples of the industrially produced esters in very large quantities.[9-13]

Esterification can be regarded as the transformation of the carboxylic acids or their derivatives into esters. Similarly, the counterpart esterification reaction: the transformation of alcohols into esters (acylation of hydroxy groups) is equally important. [14]

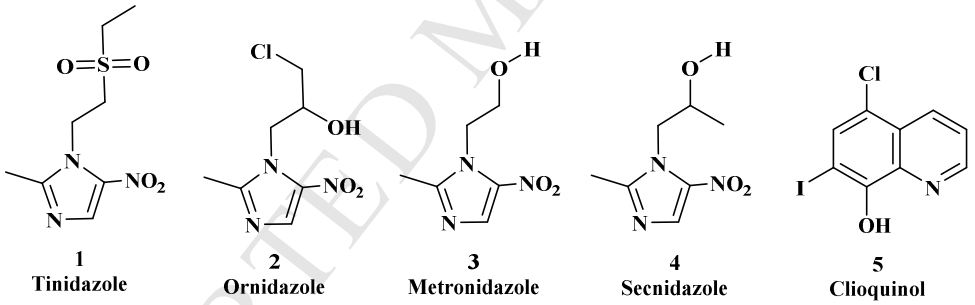

Fig. 1 Chemical structures of common 5-nitroimidazole and clioquinol

The Fig. 1 shows some 5-nitroimidazoles useful as antibiotics for the treatment of bacterial and parasitic infections. [15,16] Among these Secnidazole (Comp. 4, Fig. 1) has been explored for the treatment of amoebiasis, giardiasis, urogenital trichomoniasis and nonspecific bacterial vaginosis. A previous study proved that secnidazole is significantly faster and more effective treatment than clioquinol (Comp. 5, Fig. 1) for the patients suffering from acute intestinal amoebiasis.[17] The ester derivatives of secnidazole and other similar compounds have been synthesized by different synthetic methods to obtain novel compounds with enhanced biological

activities, improved physiochemical properties with lower toxicity values than their parent drugs. [18-21] Therefore esterification of drug molecules is highly desirable.

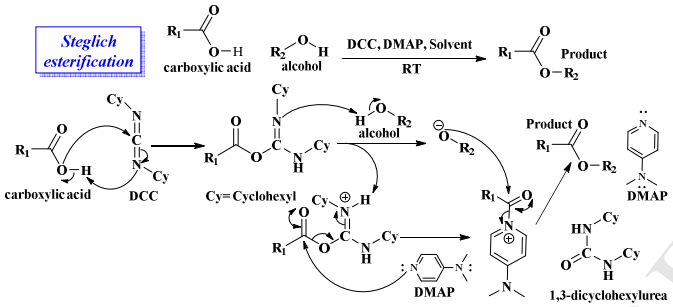

Scheme1 General reaction and mechanism of the Steglich esterification

Table 1 Safety information of DMAP, DCU and Pyridine

Material	CAS	Standard Safety Code	Symbol	Safety Information
DMAP	1122-58-3	[a]GHS06		[a]Acute toxicity (oral, dermal, inhalation, Categ: 1,2,3)
DCU	2387-23-7	[a]GHS07 [b]H411		[a]Acute toxicity(oral, dermal, inhalation, Categ: 4) [b]Toxic to aquatic life with long lasting effects
Pyridine	110-86-1	[a]GHS07		[a]Acute toxicity (oral, dermal, inhalation, Categ: 4)

Source: [a]www.sigmaaldrich.com, [b]www.caymaneurope.com

There are many catalysts or reagents used for the esterification (acids, lewis acids). [22,23] For an example, the Steglich esterification reaction is a versatile (Scheme 1) method which uses the combination of DCC (dicyclohexylcarbodiimide) and DMAP (Dimethlyaminopyridine).[24-27] Previously this method has been utilized [28] for the esterification of secnidazole with the following molar ratios, Secnidazole: Bromobenzoic acid:DCC:DMAP = 3:3.3:3.3:0.2 (mmol) in CH_2Cl_2 at room temperature, for 12 h and resulting product (ester) was purified through column chromatography (ethylacetate:petroleum ether = 1:1) in 88% yield. Similar reactions reported by other researchers indicate that yields can vary between 53-73%. [18,19] The mechanism of Steglich reaction [29,30] shows that there can be two possible materials left (Scheme 1) after the product (ester) formation is complete. The two byproducts DMAP and 1,3-dicyclohexylurea (DCU) possess acute toxicity (Table 1). This shows threat to the environment will be much higher if we apply Steglich

reaction on an industrial scale. Therefore less toxic esterification methods are highly desirable.

The easier availability of carboxylic acids allows easier excess to the corresponding acid-chlorides. Therefore we have utilized the carboxylic acid-chlorides to esterify (one-pot reaction) the Secnidazole (alcohol component) in presence of pyridine present in toluene (solvent/catalyst system). The HCl released during the reaction can be easily neutralized by a glass-u-tube connected with a conical flask containing aqueous NaOH. This leaves pyridine in the reaction mixture, which is much less toxic when compared to the DMAP and 1,3-dicyclohexylurea. There are other two advantages, firstly the toluene/pyridine mixed solvent system is easier to recycle when compared with the DMAP, 1,3-dicyclohexylurea. Secondly, simple recrystallization gives pure product which eliminates the solvent consumption in column chromatography thereby decreases the production cost. This esterification procedure has the potential for application to other molecules.

In this manuscript we present environmentally safer synthesis of four new secnidazole ester molecules spectroscopic properties and electrochemical properties. To best of our knowledge (SCI Finder) this is first report describing a detailed synthesis, structural characterization of secnidazole esters, by the EIMS, NMR (^{1}H and ^{13}C NMR), UV-vis absorption spectroscopy and cyclic voltammetry. The details of structural properties are very important to characterize, analyze the stability and metabolism of these molecules for present and future researchers.

2. Experimental Details

2.1 General Methods and Characterization

All chemicals and solvents were of reagent grade and purchased from commercial sources and used without further purification. Secnidazole and other APIs were

provided by NabiQasim Pvt. Thin layer chromatography was performed on Merck silica gel 60F254 plates and observed under UV. Melting point was recorded in a glass capillary tube on Gallenkamp (sonyo) apparatus. FTIR spectra were recorded directly on Bruker FT-IR spectrophotometer (Vector 22) in the range of 4000-400 cm^{-1}. EIMS and HR-MS spectra were recorded on JeolMS JMS-HX-110. ^{1}H-NMR and ^{13}C-NMR were recorded on BrukerAvance500 spectrophotometers at 500 MHz for ^{1}H and 125 MHz for ^{13}C NMR. The CV spectra were recorded on CHI660 instrument.

2.2 Synthesis of 1-(2-methyl-5-nitro-1H-imidazol-1-yl)propan-2-yl-4-methylbenzoate (M1)

In a round bottom flask (fitted with dropping funnel, condenser, and a glass u-tube connected to a flask containing NaOH to neutralize the HCl) containing Secnidazole (2 g, 10.8 mmol) we added toluene (20 mL), and pyridine (2 mL). The flask was heated with stirring for 30 minutes at 70 ^{o}C. Later 4-methylbenzoylchloride (CAS: 212-864-8, Aldrich, 2 g, 12.9 mmol) was slowly added (through dropping funnel) to the flask and stirring continued at 70 ^{o}C for 4.5 h. The reaction mixture was allowed to cool and treated with saturated aqueous $NaHCO_3$ solution and water. The organic layer was separated (separatory funnel) and solvent was removed (rotary/vacuum) to obtain the product. This was recrystallized from chloroform/toluene to obtain pure white crystals in 77% yield. M.P.: 112-114 ^{o}C. ^{1}H NMR (500 MHz, DMSO-d_6): δ 7.964 (s, 1 H, imidazole H), 7.719-7.702 (d, J = 8.5 Hz, 2 H, ArH), 7.303-7.287 (d, J=8.5 Hz, 2 H, ArH), 5.461-5.398 (m, 1H, CH), 4.666-4.525 (m, 2 H, CH_2), 2.407 (s, 3 H, CH_3), 2.354 (s, 3 H, CH_3), 1.408-1.395 (d, J=6.5 Hz, 3 H, CH_3). ^{13}C NMR (125 MHz, DMSO-d_6): δ 164.68 (C=O), 151.34 (N=C), 143.95 (aromatic carbon), 138.52 (C-NO_2), 133.14, 129.31, 129.00, 126.26 (aromatic carbons), 69.09 (O-CH), 49.46 (N-CH_2), 21.10 (CH_3), 17.3 (CH_3), 13.95 (CH_3). FTIR (neat, $\bar{\upsilon}$, cm^{-1}): 3127, 3019, 2992, 2969, 2929, 2876, 1718, 1430, 1532, 1366, 1270, 1191. EIMS m/z (R.A.%): 303 (M^{+}, 5), 257 (82),

177 (4), 119 (100), 91 (20), 80 (2), 65 (5), 53 (5). HRMS [M^+] calcd. for $C_{15}H_{17}N_3O_4$ 303.1219 (found 303.1216).

2.3 Synthesis of 1-(2-methyl-5-nitro-1H-imidazol-1-yl)propan-2-yl-3,4-dimethoxybenzoate (M2)

Similar to the above procedure we added 3,4-dimethoxybenzoyl chloride (CAS: 3535-37-3, Aldrich, 5.7 mmol) to the hot solution (at 70 ^oC) of secnidazole (5.5 mmol), in toluene (20 mL) and pyridine (2 mL). The reaction mixture was allowed to cool and treated with saturated aqueous $NaHCO_3$ solution and water. The organic layer was separated (separatory funnel) and solvent was removed (rotary/vacuum) to obtain the product. This was recrystallized from chloroform/toluene to obtain pure product in 61% yield. M.P.: 115-117 ^oC. ^1H NMR (500MHz, DMSO-d_6): δ 7.969 (s, 1 H, imidazole H), 7.467-7.029 (m, 3 H, Ar H), 5.427-5.349 (m, 1 H, CH), 4.662-4.558 (m, 2 H, CH_2), 3.815 (s, 3 H, CH_3), 3.777 (s, 3H, CH_3), 2.446 (s, 3 H, CH_3), 1.405-1.389 (d, J=6.4 Hz, 3 H, CH_3). ^{13}C NMR (125 MHz, DMSO-d_6): δ 164.47 (C=O), 153.15 (O-Ar), 151.42 (O-Ar), 148.38 (N=C), 138 (C-NO_2), 133.19, 128.62, 123.09, 111.42, 111.15 (aromatic carbons), 69.08 (O-CH), 55.7, 55.45 (O-CH_3), 49.36 (N-CH_2), 17.37 (CH_3), 13.99 (CH_3). FTIR (neat, $\bar{\upsilon}$, cm^{-1}): 3122, 3079, 2960, 2934, 2874, 2860, 2841, 1703, 1531, 1437, 1357, 1269, 1188. EIMS m/z (R.A.%): 349 (M^+, 16), 303 (5), 223 (2), 182 (15), 165 (100), 151 (4), 137 (6), 111 (4), 83 (7), 80 (3), 53 (3.0), 44 (5). HRMS [M^+] calcd. for $C_{16}H_{19}N_3O_6$ 349.1268 (found 349.1281).

2.4 Synthesis of 1-(2-methyl-5-nitro-1H-imidazol-1-yl)propan-2-yl-2-(4-isobutylphenyl)propanoate (M3)

For M3, we needed the 2-(4-isobutylphenyl)propanoyl chloride which is commercially unavailable therefore, In a separate round bottom flask (fitted with distillation set up), we transformed 2-(4-isobutylphenyl)propanoic acid (commercial name ibuprofen, CAS: 15687-27-1, 1.1085 g, 5.37 mmol) to 2-(4-isobutylphenyl)propanoyl chloride by

reaction with oxalyl chloride (CAS: 79-37-8, 0.53 mL, 6.05 mmol) in 20 mL of CH_2Cl_2 and catalytic anhydrous DMF (3 mL) by stirring at room temperature for 12 h. The solvents were removed and the remaining liquid was added to a warm (70 ^oC), well stirred solution (toluene 20 mL and pyridine 2 mL, round bottom flask) of secnidazole (1 g, 5.4 mmol). After complete addition, the reaction mixture was heated for 5 h. The reaction mixture was allowed to cool and treated with saturated aqueous $NaHCO_3$ solution and water. The organic layer was separated (separatory funnel) and solvent was removed (rotary/vacuum) to obtain the product. The product was recrystallized from toluene/hexane to obtain M3 in 67 % yield. M.P.: 93-96 ^oC. ^1H NMR (500 MHz, DMSO-d_6): δ 8.021 (s, 1 H, imidazole H), 7.080-7.028 (m, 4 H, Ar H), 5.162-5.115 (m, 1 H, CH), 4.552-4.316 (m, 2 H, CH_2), 3.575-3.522 (m,1 H, CH), 2.401 (s, 2 H, CH_2), 2.382 (s, 3 H, CH_3), 1.838-1.737 (m, 1 H, CH), 1.205-1.187 (d, J= 7.2 Hz, 3 H, CH_3), 1.161-1.146 (d, J= 6 Hz, 3 H, CH_3), 0.84-0.824 (d, J=6.4 Hz, 6 H, $2CH_3$). ^{13}C NMR (125 MHz, DMSO-d_6): δ 173.14 (C=O), 151.59 (N=C), 139.79 (Aromatic carbon), 138 (C-NO_2), 137.32, 133.08, 129.05, 126.78 (Aromatic carbons), 69.25 (O-CH), 49.22 (N-CH_2), 44.12 (CH), 44.00 (CH_2), 29.50 (CH), 22.10 (CH_3), 22.08 (CH_3), 18.15 (CH_3), 16.90 (CH_3), 13.97 (CH_3). FTIR (neat, $\bar{\upsilon}$, cm^{-1}): 3130, 3051, 3011, 2984, 2956, 2928, 2867, 2845, 1736, 1531, 1429, 1377, 1264, 1195. EIMS m/z (R.A.%): 373 (M^+, 5), 356 (47), 357(19), 330 (100), 327 (2), 247 (17), 245(34), 231 (46), 232 (8), 219 (86), 188 (43), 170 (22), 168 (3), 161 (97), 145 (64), 118 (66), 105 (15), 91 (22), 80 (15), 53 (15), 42 (10). HRMS [M^+] calcd. for $C_{20}H_{27}N_3O_4$ 373.2002 (found 373.1982).

2.5 Synthesis of Bis(1-(2-methyl-5-nitro-1H-imidazol-1-yl)propan-2-yl) oxalate (M4)

In a round bottom flask (fitted with dropping funnel, condenser, and a glass u-tube connected to a flask containing Na_2CO_3 to neutralize the HCl) containing Secnidazole

(2 g, 10.8 mmol) we added toluene (20 mL), and pyridine (2 mL). The flask was heated with stirring for 30 minutes at 40 ^{o}C. Later Oxalyl chloride (CAS: 79-37-8, 5.6 mmol) was carefully added (through dropping funnel) to the flask and stirring continued at 40 ^{o}C for 2.5 h. The reaction mixture was allowed to cool and treated with saturated aqueous $NaHCO_3$ solution and water. The organic layer was separated and solvent was removed to obtain the product. The product was recrystallized by using DMF/CH_2Cl_2 to obtain 91% product.

M.P.: 201-203 ^{o}C. ^{1}H NMR (500 MHz, DMSO-d_6): δ 7.997 (s, 2 H, 2imidazole H), 5.242-5.182 (m, 2 H, 2CH), 4.636-4.404 (m, 4 H, $2CH_2$), 2.434 (s, 6 H, $2CH_3$), 1.342-1.320 (d, J=6.6 Hz, 6 H, $2CH_3$). ^{13}C NMR (125 MHz, DMSO-d_6): δ 155.376 (C=O), 151.778 (N=C), 138.452 (C-NO_2), 133.141(aromatic carbons), 72.563 (O-CH), 48.954 (N-CH_2), 16.58 (CH_3), 13.913 (CH_3). FTIR (neat, $\bar{\upsilon}$, cm^{-1}): 3129, 3020, 2990, 2945, 1741, 1528, 1429, 1372, 1267, 1191. EI-MS m/z (R.A.%): 424 (M^+, 6), 407 (43), 408 (9),378 (68), 210(2), 184(8), 168 (100), 151 (27), 137 (19), 128 (25), 111 (14), 95 (43), 80 (75), 67 (27), 53 (75), 42 (53). HRMS [M^+] calcd.for $C_{16}H_{20}N_6O_8$ 424.1337 (found 424.1347).

3. Results and Discussion

3.1 Synthesis

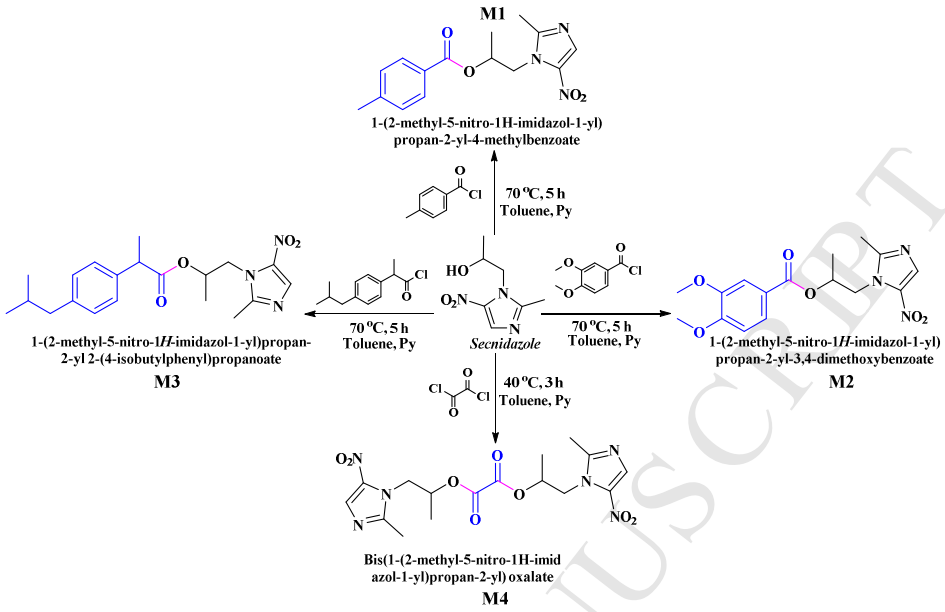

Scheme 2 Synthesis route for the secnidazole esters (M1, M2, M3 and M4)

The Scheme 2 shows the synthetic route to the secnidazole esters (M1, M2, M3 and M4). The reaction has the advantage of shorter time, when compared to the Steglich reaction applied to the secnidazole likely due to higher reactivity of carboxylic acid-chlorides.

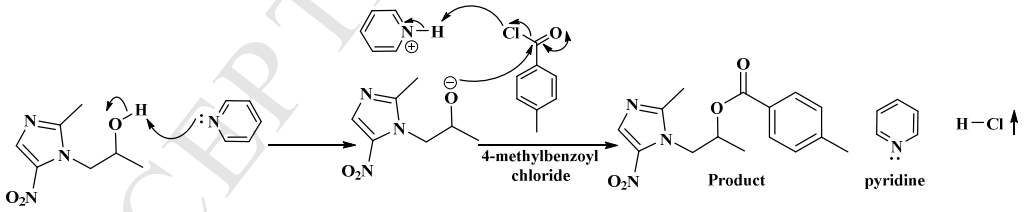

Scheme 3 Proposed esterification reaction-mechanism for the secnidazole

The products were purified by simple workup, washing with aqueous $NaHCO_3$, vacuum evaporation of solvent, and recrystallization which eliminates the solvent consumption in column chromatography thereby decreases the production cost. The other advantage is easier recycling of mixed catalytic solvent system (toluene/pyridine). The M4 shows an example in which oxalyl chloride was used instead of aromatic carboxylic acid-chloride. This reaction happens at relatively lower

temperature because of higher reactivity of oxalyl chloride. The scheme 3 shows a proposed mechanism for the esterification under the given reaction conditions. A comparison of Table 1, scheme 1 and scheme 3 shows that the reaction is relatively simple. In addition, the byproducts (pyridine and HCl) of this reaction are less toxic therefore, relatively safer for the environment when compared to the Steglich esterification reaction.

3.2 Spectroscopic Properties

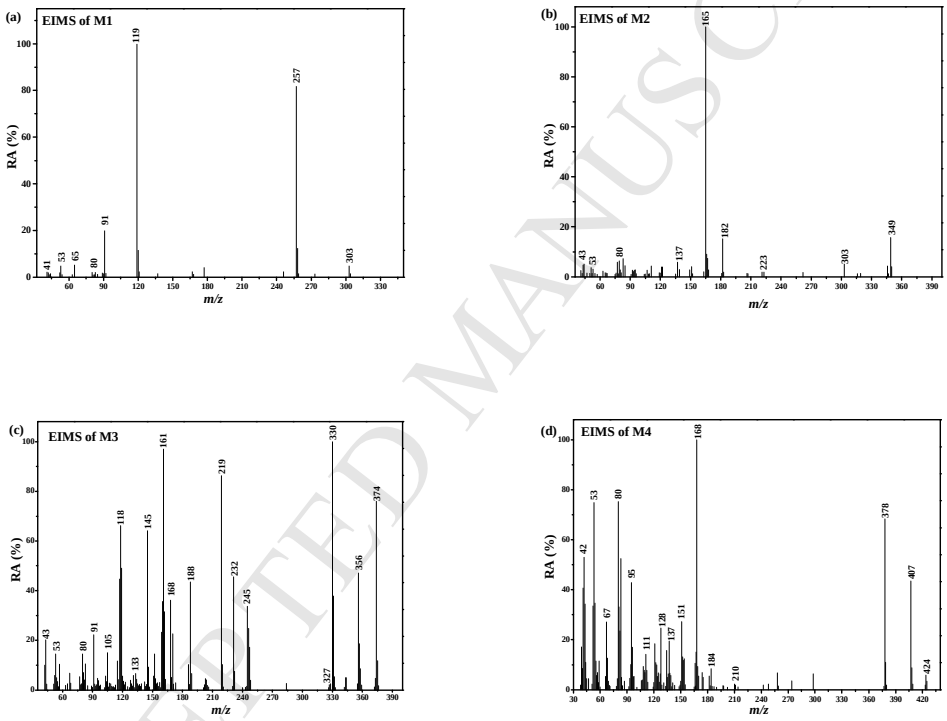

Fig. 2 EIMS of M1(a), M2(b), M3(c) and M4(d).

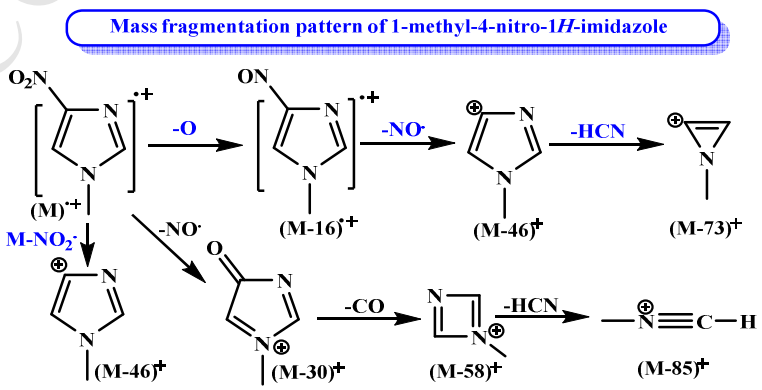

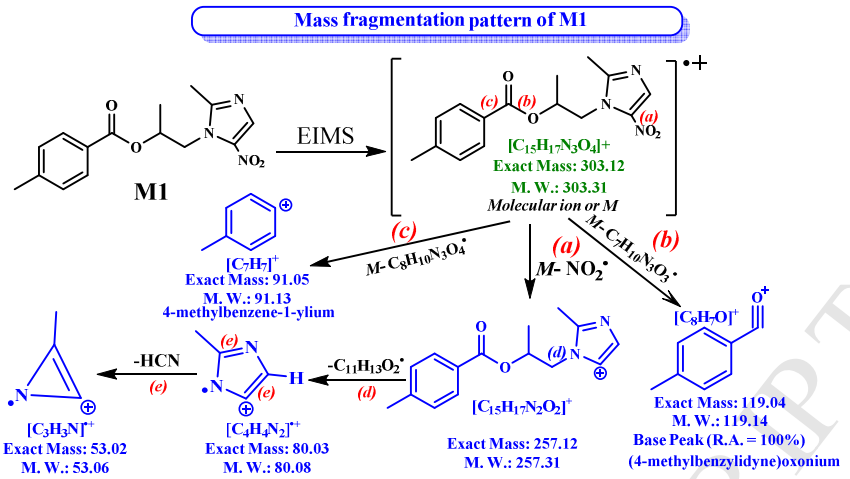

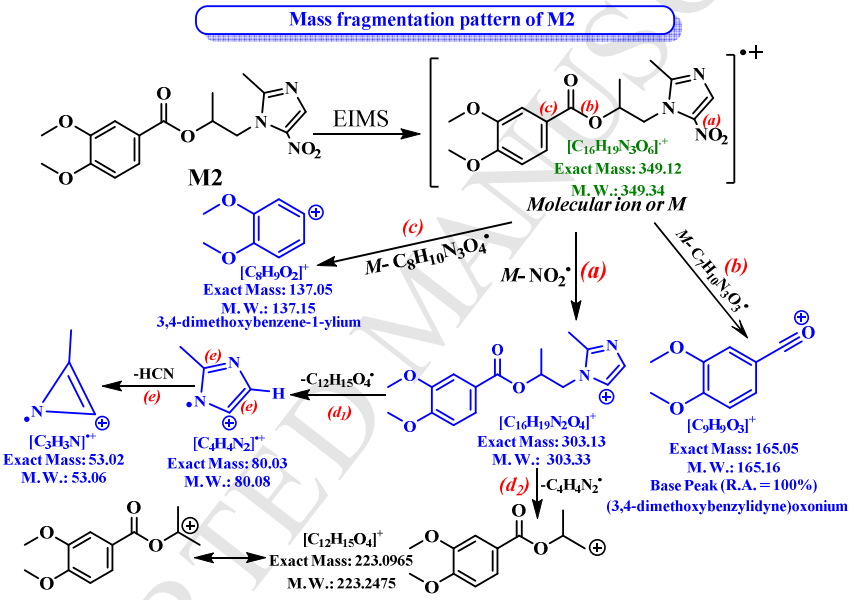

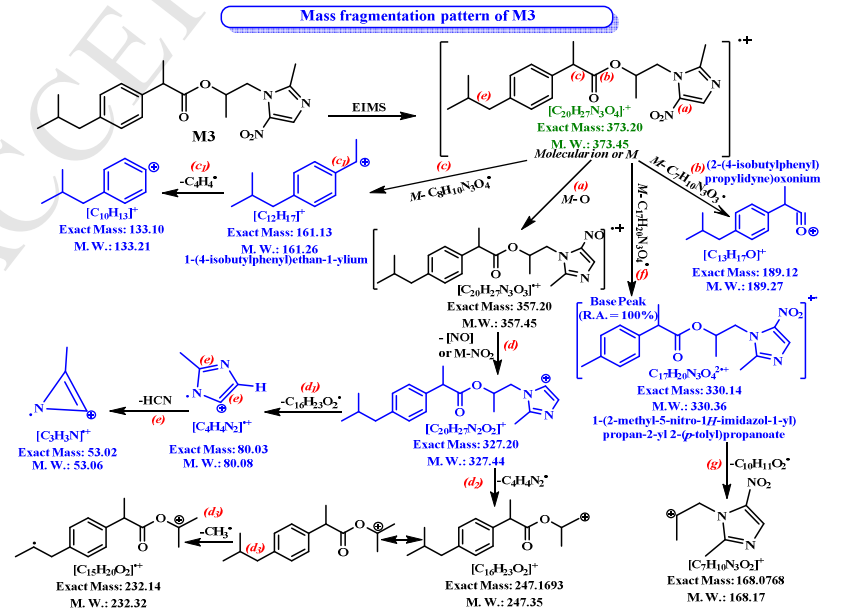

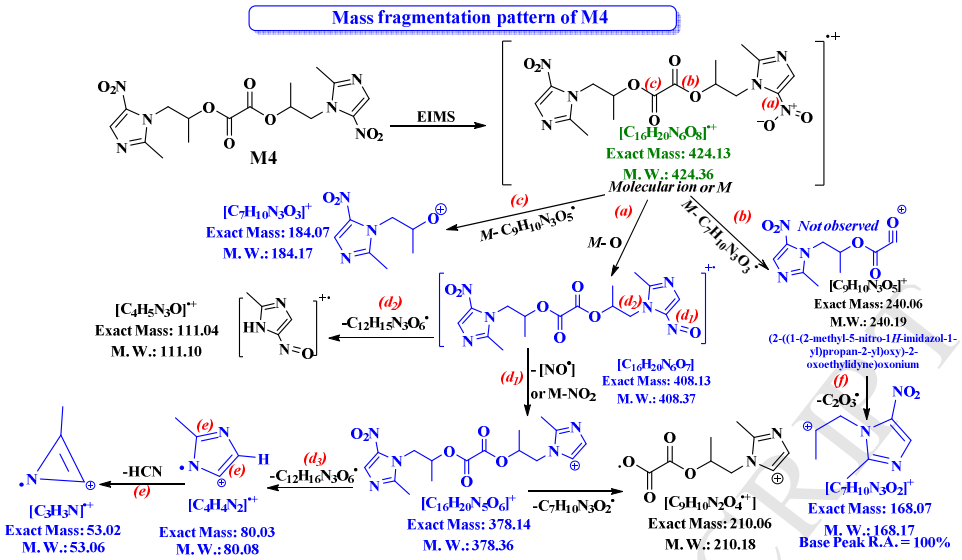

Scheme 4 EIMS fragmentation patterns of 1-methyl-4-nitro-1H-imidazole, M1, M2, M3 and M4

We studied the EIMS (Fig. 2, Fig.SA, Scheme 4), FTIR (Fig. 3, Table 2), ^{1}H-NMR (Fig.SB, Fig.4) and ^{13}C-NMR (Fig.SC, Fig.4) spectra (supporting information) to confirm the molecular structures. Although molecular structure of organic molecules could be confirmed through NMR but many research institutes and pharmaceutical industries routinely use FTIR and Mass spectrometry analysis therefore these techniques are very important for routine analysis. To best of our knowledge this is first report describing a detailed characterization of secnidazole esters, by the EIMS and NMR spectroscopy. The mass spectrometry (EIMS) provided the molecular weights (molecular ion peaks or *M*) of four compounds equal to the calculated molecular weights. The EIMS spectra indicate characteristic fragmentation patterns (Scheme 4). To understand the fragmentation patterns of four ester molecules we first studied the fragmentation pattern of the 1-methyl-4-nitro-1H-imidazole [31-33] and different ester molecules (Scheme 4).We have observed some similarities (highlighted in blue color) found in the fragmentation patterns useful to identify these molecules. The important EIMS peaks showed unique contribution of heteroatom bonds. The important peaks in the EIMS appear due to the loss of single electron, loss of HCN, M-O, M-NO, M-NO_2, M-$C_7H_{10}N_3O_3$, and M-$C_8H_{10}N_3O_4$. The comparison of fragmentation

patterns (M1, M2, M3 and M4) clearly indicate that nitroimidazoles and ester linkages can be easily confirmed through EIMS. The fragmentation patterns will greatly help in future to fast identify and analyze these molecules.[33]

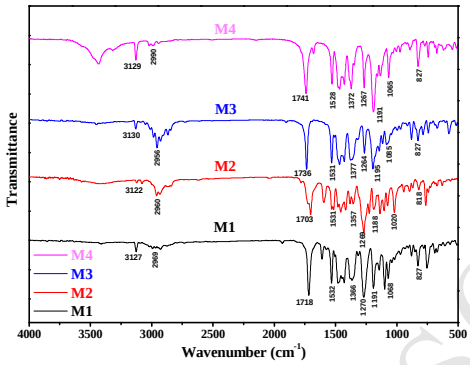

Fig. 3 FTIR of M1, M2, M3 and M4

Table 2 FTIR Characterization

Functional Groups	Secnidazole (cm^{-1})	M1 (cm^{-1})	M2 (cm^{-1})	M3 (cm^{-1})	M4 (cm^{-1})
Ar-H str.	3133	3127, 3019	3122, 3079,	3130, 3051, 3011	3129, 3020
Alk-CH str.	2918, 2896	2992, 2969, 2929, 2876	2960, 2934, 2874, 2860, 2841	2984, 2956, 2928, 2867, 2845	2990, 2945
C=O (ester)	-	1718	1703	1736	1741
C=N str.(imidazole)	1430	1430	1437	1429	1429
Ar-NO_2 (sym./asym. str.)	1538, 1367	1532, 1366	1531,1357	1531, 1377	1528, 1372
C-N, C-O	1264, 1184	1270, 1191	1269, 1188	1264,1195	1267, 1191

We have compared the important FTIR peaks of the four products (Table 2) with the previously known FTIR of secnidazole (starting material) to identify esterification and presence of other functional groups.[34,35] Similar to the secnidazole (3133 cm^{-1}) the Ar-H stretching vibrations at 3127, 3122, 3130, 3129 cm^{-1} can be assigned to the imidazole aromatic ring of the M1, M2, M3 and M4 respectively. Since after esterification the molecular structure gets additional aromatic rings so we observed additional weak bands 3079-3011 cm^{-1} due to the Ar-H stretching. A series of Alkyl-C-H stretching vibrations (2992-2841 cm^{-1}) were observed for the four compounds. The ester formation can be recognized by the C=O functional group observed at 1718, 1703, 1736 and 1741 cm^{-1} for the M1, M2, M3 and M4 respectively. The $–NO_2$ group of secnidazole shows two bands (1538, 1367 cm^{-1}) due to symmetric and asymmetric

stretches. Similarly we observed Ar-NO_2 group of the M1, M2, M3 and M4 showing two peaks respectively at 1532-1366, 1531-1357, 1531-1377, 1528-1372 cm^{-1}. The secnidazole shows two vibrations (1264, 1184 cm^{-1}) for the C-N stretches; similar bands were observed (1270-1188 cm^{-1}) for the 4 ester molecules. This region is common with the vibration region of C-O therefore there is chance of overlapped bands.

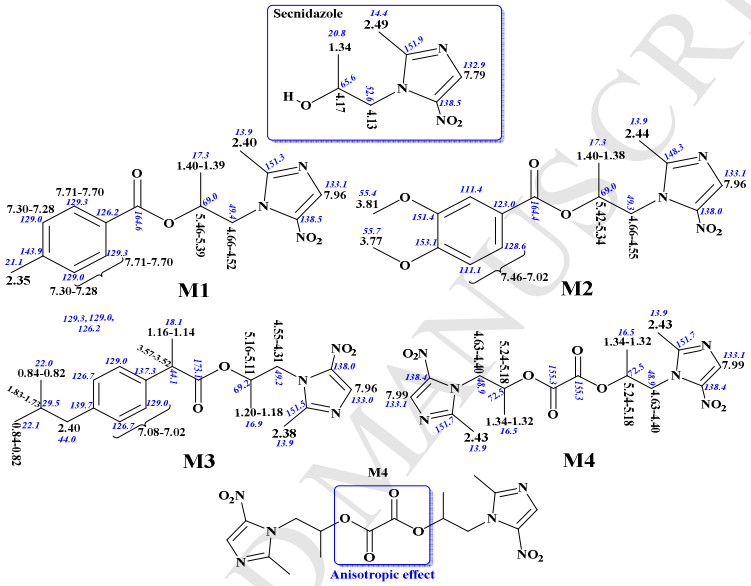

Fig. 4 ^{1}H NMR (500 MHz, DMSO-d_6) and ^{13}C NMR (125 MHz, DMSO-d_6) chemical shift values

The Fig. 4 shows the ^{1}H NMR (500 MHz, DMSO-d_6) and ^{13}C NMR (125 MHz, DMSO-d_6, DEPT 90, DEPT 135) characterization for the different positions of the M1, M2, M3 and M4 structures. The bold numbers (black) show the ^{1}H NMR chemical shift values while italic (blue) numbers indicate the ^{13}C NMR chemical shift values.

The NMR chemical shift values of secnidazole part can be characterized by the reported NMR chemical shift values of secnidazole (Fig. 4). [36,37] The other part can be characterized through NMR analysis [38], experimental results (supporting information) and comparison with predicted ^{13}C NMR chemical shift values (ChemBioDraw Ultra 14.0, MestReNova 6.1) as summarized in Table 3.

Table 3 ^{13}C NMR Characterization

Material	Predicted ^{13}C NMR (ChemBioDraw Ultra 14.0)	Experimental ^{13}C NMR	Predicted ^{13}C NMR (MestReNova 6.1)
Secnidazole	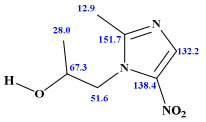	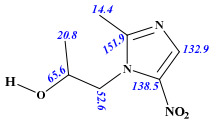	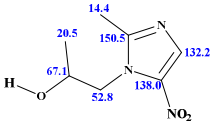
M1	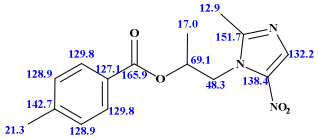	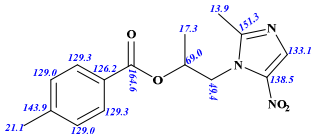	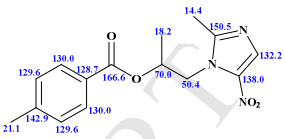
M2	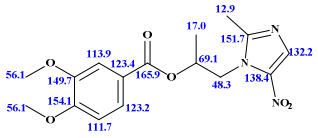	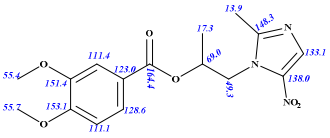	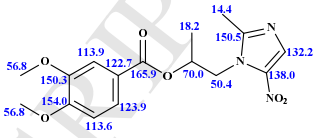
M3	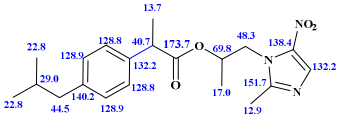	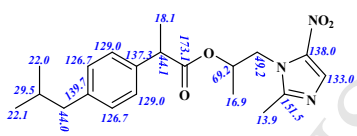	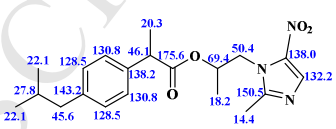
M4	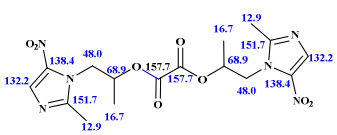	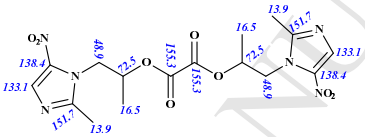	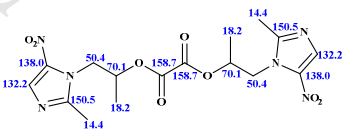

The comparison of ^{13}C NMR predicted chemical shift values with the experimental (Table 3) showed that ChemBioDraw Ultra 14.0 is more capable of predicting aromatic or sp^2 carbons, while MestReNova 6.1 predicts sp^3 hybrid carbons more accurately. Therefore the two software programs provided useful information. The details of NMR chemical shift values are given in the experimental section. The ^{13}C NMR chemical shift values of C=O (ester) for M1, M2, M3 and M4 respectively appear at 164.6, 164.4, 173.1 and 155.3 ppm. The higher variation is due to different neighbours of C=O (ester) imparting different inductive and mesomeric effects. To best of our knowledge ^{13}C NMR value 155.3 ppm for the C=O (ester, M4) is rarely observed in scientific literature. The lower ^{13}C NMR value of C=O (155.3 ppm) is likely due to the adjacent oxygen atoms and the anisotropic effect (directionally dependentπ-electron density distribution) from the adjacent C=O group [39, 40] making the carbon more shielded, thereby moving the NMR chemical shift values

relatively upfield. The ArC-NO_2 appears in the range 138.5-138.0 ppm which shows very small variation likely because NMR chemical shift values of the imidazole ring show minor change.

3.3 Optical and Electrochemical Properties

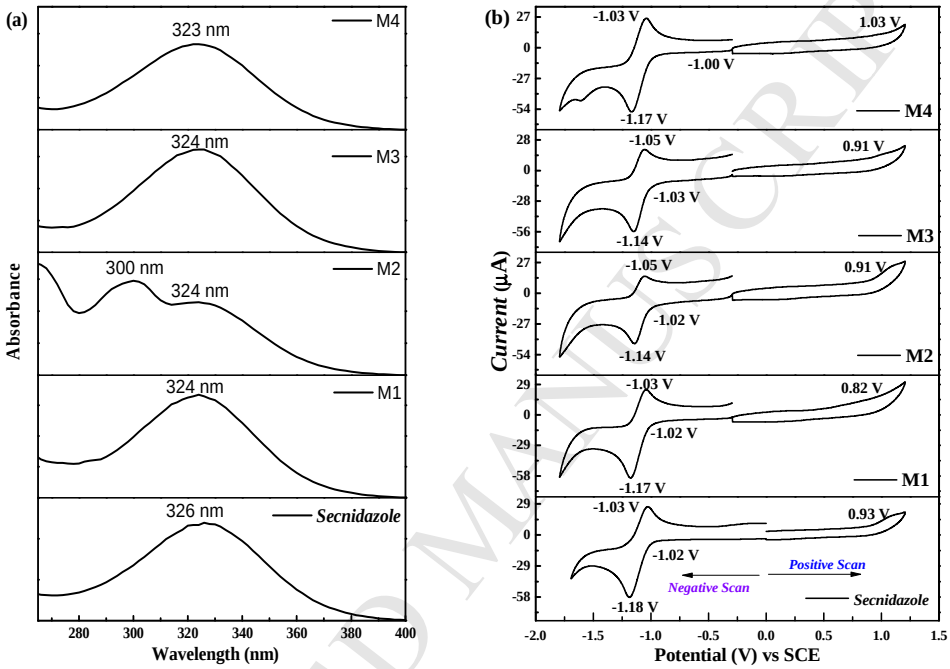

Fig. 5 UV-vis absorbance spectra (a) and Cyclic voltammograms (b) of the Secnidzole, M1, M2, M3 and M4

Table 4 Summary of UV-vis and Electrochemical Properties

Molecule	UV-vis λ_{max} (nm)	$^{a}E_g^{opt}$ (eV)	$^{b}E_{ox}$ (V) /E_{HOMO} (eV)^{c} (negative Scan)	Reversibility (positive scan)	$^{b}E_{red}$ (V) /E_{LUMO} (eV)^{c} (negative Scan)	$^{d}E^{0'}$ Formal Potential (negative Scan) (V)	^{e}Reversibility (negative scan) $i_{p,r}$ /$i_{p,f}$
Secnidazole	326	3.229	0.93/5.33	NO	-1.02/3.38	-1.104	0.89
M1	324	3.271	0.82/5.22	NO	-1.02/3.38	-1.106	0.84
M2	300, 324	3.289	0.91/5.31	NO	-1.02/3.38	-1.098	0.82
M3	324	3.280	0.91/5.31	NO	-1.03/3.37	-1.101	0.92
M4	323	3.271	1.03/5.43	NO	-1.00/3.40	-1.103	0.95

1. [a] Optical band gap, $E_g^{opt} = 1240/\lambda_{onset}$
2. [b] *Onset*-peak potentials *vs. SCE*.
3. [c] Energy levels are estimated from $E_{HOMO/LUMO} = -(E_{ox/red} + 4.4)$ eV.
4. [d] $E^{0'} = E_{p,f} + E_{p,r}/2$; $E_{p,f}$ and $E_{p,r}$ represent the forward and reverse peak potentials.
5. [e] $i_{p,r}$ /$i_{p,f}$ = 1, reversible

The UV-vis absorbance spectra of secnidazole and ester molecules were measured in DMSO (Fig. 5a) and the data is summarized in Table 4. The UV-vis spectra showed broad bands [41] with λ_{max} = 326, 324, (300, 324), 324, 323 nm for the secnidazole, M1, M2, M3 and M4 respectively attributed to the π-π* electronic transition of the aromatic ring. A new band at 300 nm observed for M2 can be attributed to the dimethoxybenzene. From the onset of spectra we calculated the optical band gap (E_g^{opt}) of these molecules about 3.2 eV.

Electrochemical properties of Secnidzole, M1, M2, M3 and M4 were investigated by the cyclic voltammetry (CV, DMSO solvent, WE: GC, CE: Pt wire, and Bu_4NClO_4 as electrolyte) at the scan rate = 0.1 V/s (Fig.5b, Table 4). It is well known that If a reduced/oxidized molecule is stable (time scale of the experiment) in solution and there is reversible electron transfer reactions in both directions (forward/reverse) then the peak current observed for the return potential scan ($i_{p,r}$) should be equal ($i_{p,r}/i_{p,f}$ = 1) to that seen for the forward potential scan ($i_{p,f}$) in a cyclic voltammetry experiment. All the molecules showed $i_{p,r}/i_{p,f}$ close to 1 (Table 4) for the negative scan, therefore we conclude that they undergo reversible reduction process. This occurs due to one electron reduction of the nitro (–NO_2) group attached to the imidazole ring (R-NO_2 + $e^- \rightleftharpoons RNO_2^{\bullet -}$). [42,43] The metabolism mechanism studies have shown that this is an essential property required for the anti-bacterial (anti-protozoal) activity of the secnidazole and related molecules. [20]

An irreversible oxidation process (+ve scan, Fig. 5b) was observed (onset oxidation potentials, E_{ox} vs *SCE*) at 0.93, 0.82, 0.91, 0.91, and 1.03 V for the secnidazole, M1, M2, M3 and M4 respectively. From the oxidation potential values, the HOMO energy levels (E_{HOMO}) were calculated (5.33, 5.22, 5.31, 5.31, and 5.43 eV). Similarly from

the onset reduction potentials values (Table 4), the calculated LUMO energy levels (E_{LUMO}) are 3.38, 3.38, 3.38, 3.37, and 3.40 eV respectively.

4. Conclusions

In summary, we have synthesized four new secnidazole esters. The reactions provided moderate to very good yields. The esterification procedure is less toxic, products are easy to purify, solvent system (toluene/pyridine) can be recycled therefore has higher environmental safety and experimental simplicity. The structures were studied by the EIMS, FTIR, ^{1}H NMR, ^{13}C NMR, UV-vis absorption and cyclic voltammetry. The important EIMS peaks showed unique contribution of heteroatom bonds. These peaks originate from the loss of single electron, loss of HCN, M-O, M-NO, M-NO_2, M-$C_7H_{10}N_3O_3$, and M-$C_8H_{10}N_3O_4$. The comparison of EIMS fragmentation patterns indicate that nitroimidazole and ester linkages (heteroatom linkages) can be confirmed through the EIMS. This will greatly help to fast identify and analyze these molecules. The comparison of ^{13}C NMR predicted values with the experimental values showed that ChemBioDraw Ultra 14.0 has advantage of predicting aromatic or sp^2 carbons, while MestReNova 6.1 predicts sp^3 hybrid carbons more accurately. Therefore the two software programs provided useful information. The electrochemical properties indicated an irreversible oxidation process and reversible reduction process in the four ester molecules similar to the parent secnidazole. The HOMO energy levels (E_{HOMO}) are 5.33, 5.22, 5.31, 5.31, and 5.43 eV (secnidazole, M1, M2, M3 and M4). Similarly the LUMO energy levels (E_{LUMO}) are 3.38, 3.38, 3.38, 3.37, and 3.40 eV respectively.

Acknowledgements We highly acknowledge the National Natural Science Foundation of China (Grant Number: 21374044) and HEC Pakistan for supporting this research work.

Supplementary Data Spectroscopic Spectral data related to this article is available in the online supporting information.

References

[1] K. Ishihara, S. Ohara, H. Yamamoto, Direct Condensation of Carboxylic Acids with Alcohols Catalyzed by Hafnium(IV) Salts, Science 290 (5494) (2000) 1140-1142. http://dx.doi.org/10.1126/science.290.5494.1140

[2] E. Wang, X. Ma, S. Tang, R. Yan, Y. Wang, W. W. Riley, M. J. T. Reaney, Synthesis and oxidative stability of trimethylolpropane fatty acid triester as a biolubricant base oil from waste cooking oil, Biomass Bioenergy 66 (2014) 371-378. http://dx.doi.org/10.1016/j.biombioe.2014.03.022

[3] S. Bagheri, N. M. Julkapli, W. A. Yehye, Catalytic conversion of biodiesel derived raw glycerol to value added products, Renew. Sustainable Energy Rev. 41 (2015) 113-127. http://dx.doi.org/10.1016/j.rser.2014.08.031

[4] A. Behr, J. Eilting, K. Irawadi, J. Leschinski, F. Lindner, Improved utilisation of renewable resources: New important derivatives of glycerol, Green Chem. 10 (1) (2008) 13-30. http://dx.doi.org/10.1039/B710561D

[5] C.-M. Yang, L. O. Luedecke, B. G. Swanson, Inhibition of Microorganisms In Salad Dressing By Sucrose And Methylglucose Fatty Acid Monoesters, J. Food Process Preserv. 27 (4) (2003) 285-298. http://dx.doi.org/10.1111/j.1745-4549.2003.tb00518.x

[6] F. Shahidi, Y. Zhong, Novel antioxidants in food quality preservation and health promotion, Eur. J. Lipid Sci. Technol. 112 (9) (2010) 930-940. http://dx.doi.org/10.1002/ejlt.201000044

[7] S. Verma, A. Singh, A. Mishra, Gallic acid: molecular rival of cancer, Environ.Toxicol. Pharmacol. 35 (3) (2013) 473-485. http://dx.doi.org/10.1016/j.etap.2013.02.011

[8] C. Locatelli, F. B. Filippin-Monteiro, T. B. Creczynski-Pasa, Alkyl esters of gallic acid as anticancer agents: A review, Eur. J. Med. Chem. 60 **(**2013) 233-239. http://dx.doi.org/10.1016/j.ejmech.2012.10.056

[9] C. Vilela, A. F. Sousa, A. C. Fonseca, A. C. Serra, J. F. J. Coelho, C. S. R. Freire, A. J. D. Silvestre, The quest for sustainable polyesters – insights into the future, Polym. Chem. 5 (9) (2014) 3119-3141. http://dx.doi.org/10.1039/C3PY01213A

[10] Y. Jiang, A. J. J. Woortman, G. O. R. Alberda van Ekenstein, K. Loos, Environmentally benign synthesis of saturated and unsaturated aliphatic polyesters via enzymatic polymerization of biobased monomers derived from renewable resources, Polym. Chem. 6 (30) (2015) 5451-5463. http://dx.doi.org/10.1039/C5PY00660K

[11] H. Lee, M. Yanilmaz, O. Toprakci, K. Fu, X. Zhang, A review of recent developments in membrane separators for rechargeable lithium-ion batteries, Energy Environ. Sci. 7 (12) (2014) 3857-3886. http://dx.doi.org/10.1039/C4EE01432D

[12] A. E. Nemr, S. Ragab, A. E. Sikaily, Testing zinc chloride as a new catalyst for direct synthesis of cellulose di- and tri-acetate in a solvent free system under microwave irradiation, Carbohydr. Polym. 151 (2016) 1058-1067. http://dx.doi.org/10.1016/j.carbpol.2016.06.072

[13] U. Heudorf, V. Mersch-Sundermann, J. Angerer, Phthalates: Toxicology and exposure, Int. J. Hyg. Environ. Health. 210 (5) (2007) 623-634. http://dx.doi.org/10.1016/j.ijheh.2007.07.011

[14] S.-Q. Liu, R. Holland, V. L. Crow, Esters and their biosynthesis in fermented dairy products: a review, Int. Dairy J. 14 (11) (2004) 923-945. http://dx.doi.org/10.1016/j.idairyj.2004.02.010

[15] L. Zhang, X. M. Peng, G. L. V. Damu, R. X. Geng, C. H. Zhou, Comprehensive Review in Current Developments of Imidazole-Based Medicinal Chemistry, Med. Res. Rev. 34 (2) (2014) 340-437. http://dx.doi.org/10.1002/med.21290

[16] A. Mital, Synthetic Nitroimidazoles: Biological Activities and Mutagenicity Relationships, Sci. Pharm. 77 (3) (2009) 497-520. http://dx.doi.org/10.3797/scipharm.0907-14

[17] J. C. Gillis, L. R. Wiseman, Secnidazole, Drugs 51 (4) (1996) 621-638. http://dx.doi.org/10.2165/00003495-199651040-00007

[18] Y. Li, C. P. Zhao, H. P. Ma, M. Y. Zhao, Y. R. Xue, X. M. Wang, H. L. Zhu, Design, synthesis and antimicrobial activities evaluation of Schiff base derived from secnidazole derivatives as potential FabH inhibitors, Bioorg. Med. Chem. 21 (11) (2013) 3120-3126. http://dx.doi.org/10.1016/j.bmc.2013.03.023

[19] H. J. Zhang, D. D. Zhu, Z. L. Li, J. Sun, H. L. Zhu, Synthesis, molecular modeling and biological evaluation of β-ketoacyl-acyl carrier protein synthase III (FabH) as novel antibacterial agents, Bioorg. Med. Chem. 19 (15) (2011) 4513-4519. http://dx.doi.org/10.1016/j.bmc.2011.06.021

[20] M. C. Chung, P. L. Bosquesi, J. L. dos Santos, A Prodrug Approach to Improve the Physico-Chemical Properties and Decrease the Genotoxicity of Nitro Compounds, Curr. Pharm. Des. 17 (32) (2011) 3515-3526. http://dx.doi.org/10.2174/138161211798194512

[21] E. I. Parkinson, M. J. Hatfield, L. Tsurkan, J. L. Hyatt, C. C. Edwards, L. D. Hicks, B. Yan, P. M. Potter, Requirements for mammalian carboxylesterase inhibition by substituted ethane-1,2-diones, Bioorg. Med. Chem. 19 (15) (2011) 4635-4643. http://dx.doi.org/10.1016/j.bmc.2011.06.012

[22] S. L. Barbosa, G. R. Hurtado, S. I. Klein, V. L. Junior, M. J. Dabdoub, C. F. Guimaraes, Niobium to alcohol mol ratio control of the concurring esterification and etherification reactions promoted by $NbCl_5$ and Al_2O_3 catalysts under microwave irradiation
Appl. Catal., A 338 (1) (2008) 9-13. http://dx.doi.org/10.1016/j.apcata.2007.12.013

[23] H. N. Roy, A. H. Al Mamun, Regiospecific Phenyl Esterification to Some Organic Acids Catalyzed by Combined Lewis Acids, Synth. Commun. 36 (20) (2006) 2975-2981. http://dx.doi.org/10.1080/00397910600773759
[24] B. Neises, W. Steglich, Simple Method for the Esterification of Carboxylic Acids, Angew. Chem. Int. Ed. 17 (7) (1978) 522-524. http://dx.doi.org/10.1002/anie.197805221
[25] A. Hassner, V. Alexanian, Direct room temperature esterification of carboxylic acids, Tetrahedron Lett. 19 (46) (1978) 4475-4478. http://dx.doi.org/10.1016/S0040-4039(01)95256-6
[26] C. K. Z. Andrade, R. O. Rocha, O. E. Vercillo, W. A. Silva, R. A. F. Matos, DCC/DMAP-Mediated Coupling of Carboxylic Acids with Oxazolidinones and Thiazolidinethiones, Synlett. 2003 (15) (2003) 2351-2352. http://dx.doi.org/10.1055/s-2003-42117
[27] N. N. Farshori, M. R. Banday, Z. Zahoor, A. Rauf, DCC/DMAP mediated esterification of hydroxy and non-hydroxy olefinic fatty acids with β-sitosterol: In vitro antimicrobial activity, Chin. Chem. Lett. 21 (6) (2010) 646-650. http://dx.doi.org/10.1016/j.cclet.2010.01.003
[28] P. Tian, J. S. Peng, Z. Y. Li, G. Q. Lin, Lipase-Catalyzed Resolutions of both Enantiomers of Ornidazole and Secnidazole, Chin. J. Chem. 21 (7) (2003) 853-857. http://dx.doi.org/10.1002/cjoc.20030210727
[29] H. Wiener, An improved method for the catalytic preparation of t-butyl esters of carboxylic and fatty acids, J. Mol. Catal. 37 (1) **(**1986) 45-52. http://dx.doi.org/10.1016/0304-5102(86)85136-7
[30] S. Xu, I. Held, B. Kempf, H. Mayr, W. Steglich, H. Zipse, The DMAP-Catalyzed Acetylation of Alcohols—A Mechanistic Study (DMAP=4 (Dimethylamino)pyridine, Chem. Eur. J. 11 (16) (2005) 4751. http://dx.doi.org/10.1002/chem.200500398

[31] W. C. M. M. Luijten, J. V. Thuijl, Mass spectrometry of nitroazoles 1–The mass spectra of methyl substituted nitropyrazoles, J. Mass. Spectrom. 14 (11) (1979) 577-584. http://dx.doi.org/10.1002/oms.1210141102
[32] W. C. M. M. Luijten, J. V. Thuijl, Mass spectrometry of nitroazoles: 2—the mass spectra of methyl substituted nitroimidazoles, J. Mass. Spectrom. 16 (5) (1981) 199-208. http://dx.doi.org/10.1002/oms.1210160504
[33] L. F. Capitan-Vallvey, A. Ariza, R. Checa, N. Navas, Liquid Chromatography-Mass Spectrometry Determination of Six 5-Nitroimidazoles in Animal Feedstuff, Chromatographia 65 (5) (2007) 283-290. http://dx.doi.org/10.1365/s10337-006-0147-9
[34] S. Mishra, D. Chaturvedi, P. Tandon, V. P. Gupta, A. P. Ayala, S. B. Honorato, H. W. Siesler, Molecular Structure and Vibrational Spectroscopic Investigation of Secnidazole Using Density Functional Theory, J. Phys. Chem. A. 113 (1) (2009) 273-281. http://dx.doi.org/10.1021/jp805399h
[35] S. Demirayak, A. C. Karaburun, N. Kiraz, Synthesis and antibacterial activities of some 1-[2-(substituted pyrrol-1-yl)ethyl]-2-methyl-5-nitroimidazole derivatives, Eur. J. Med. Chem. 34 (3) (1999) 275-278. http://dx.doi.org/10.1016/S0223-5234(99)80062-2
[36] R. Chadha, D.V.S. Jain, A. Aggarwal, S. Singh, D. Thakur, Binding constants of inclusion complexes of nitroimidazoles with β-cyclodextrins in the absence and presence of PVP, Thermochim. Acta 459 (1) (2007) 111-115. http://dx.doi.org/10.1016/j.tca.2007.04.016
[37] T. C. Ramalho, M. Bühl, Probing NMR parameters, structure and dynamics of 5-nitroimidazole derivatives. Density functional study of prototypical radiosensitizers, Magn. Reson. Chem. 43 (2) (2005) 139-146. http://dx.doi.org/10.1002/mrc.1514
[38] D. L. Pavia, G. M. Lampman, G. S. Kriz, J. R. Vyvyan, Introduction to Spectroscopy, 2009, 4th ed.; Brooks/Cole, Cengage Learning: Belmont, CA, USA.
[39] R. J. Abraham, N. J. Ainger, Proton chemical shifts in NMR. Part 13. Proton chemical shifts in ketones and the magnetic anisotropy and electric field effect of the carbonyl group,
J. Chem. Soc., Perkin Trans. 2 (3) (1999) 441-448. http://dx.doi.org/10.1039/A808908F
[40] R. J. Abraham, M. Mobli, R. J. Smith, ^{1}H chemical shifts in NMR: Part 19. Carbonyl anisotropies and steric effects in aromatic aldehydes and ketones, Magn. Reson. Chem. 41 (1) (2003) 26-36. http://dx.doi.org/10.1002/mrc.1125
[41] A. B. Rivera, R. G. Hernández, H. N. de Armas, D. M. C. Elizástegi, M. V. Losada, Physico-chemical and solid-state characterization of secnidazole II Farmaco. 55 (11), (2000) 700-707. http://dx.doi.org/10.1016/S0014-827X(00)00096-3
[42] A. Radi, S. El-Laban, A. G. El-Kourashy, Electrochemical reduction of secnidazole and its determination in tablets, Electroanal. 9 (8) (1997) 625-628. http://dx.doi.org/10.1002/elan.1140090809
[43] C. Yañez, J. Pezoa, M. Rodríguez, L. J. Núñez-Vergara, J. A. Squella, Voltammetric Behavior of a 4-Nitroimidazole Derivative Nitro Radical Anion Formation and Stability,
J. Electrochem. Soc. 152 (6) (2005) J46-J51. http://dx.doi.org/10.1149/1.1904983

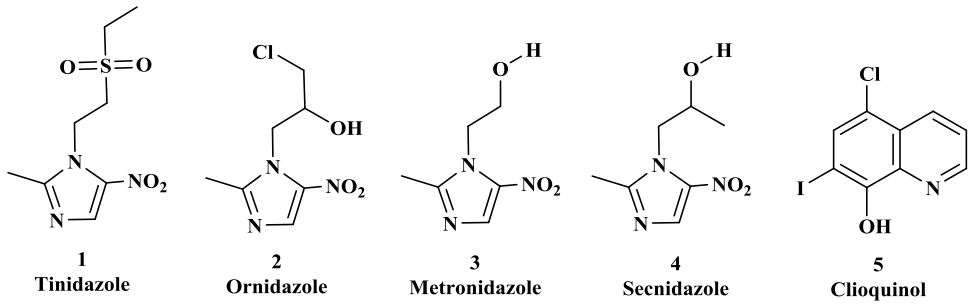

Fig. 1 Chemical structures of common 5-nitroimidazole and clioquinol

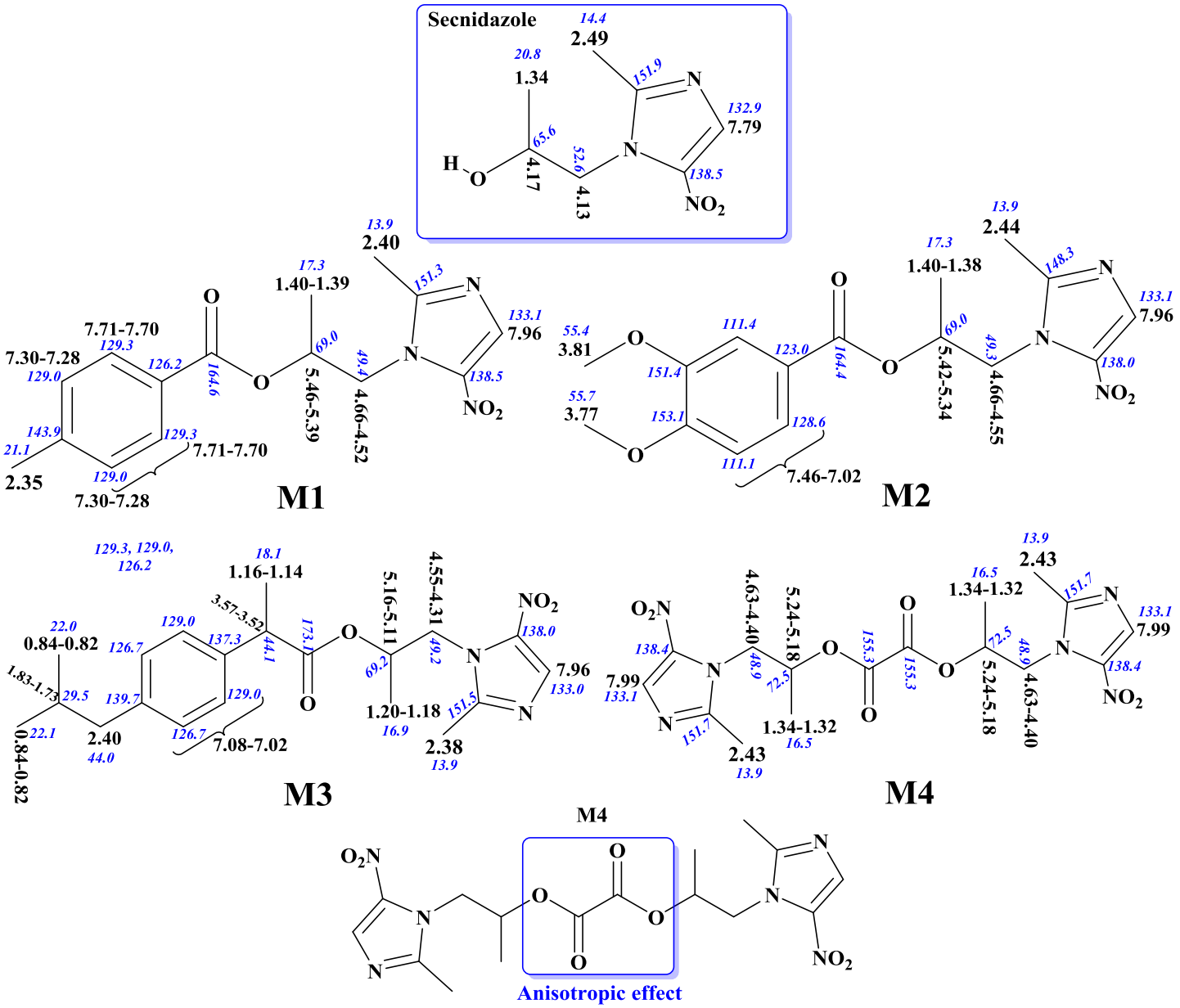

Fig. 4 ^{1}H NMR (500 MHz, DMSO-d_6) and ^{13}C NMR (125 MHz, DMSO-d_6) chemical shift values

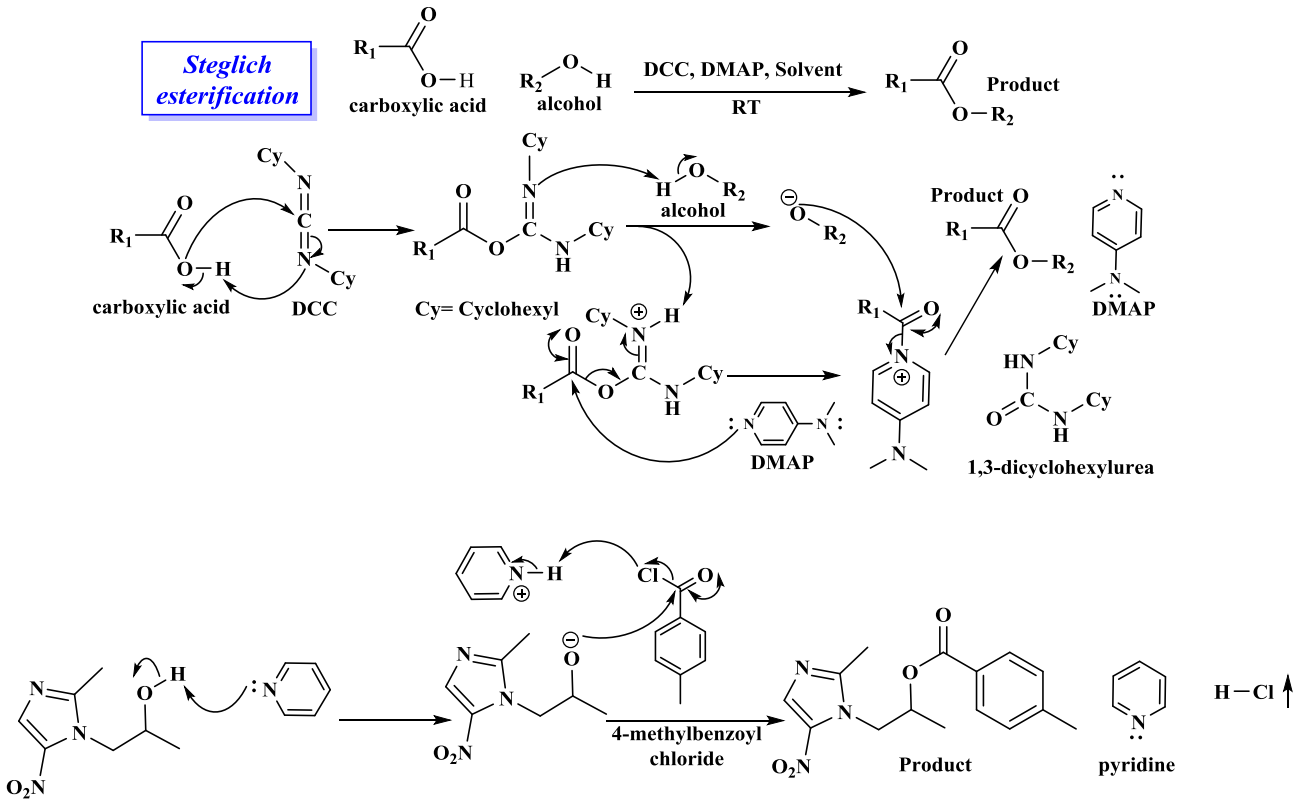

Scheme1 General reaction and mechanism of the Steglich esterification

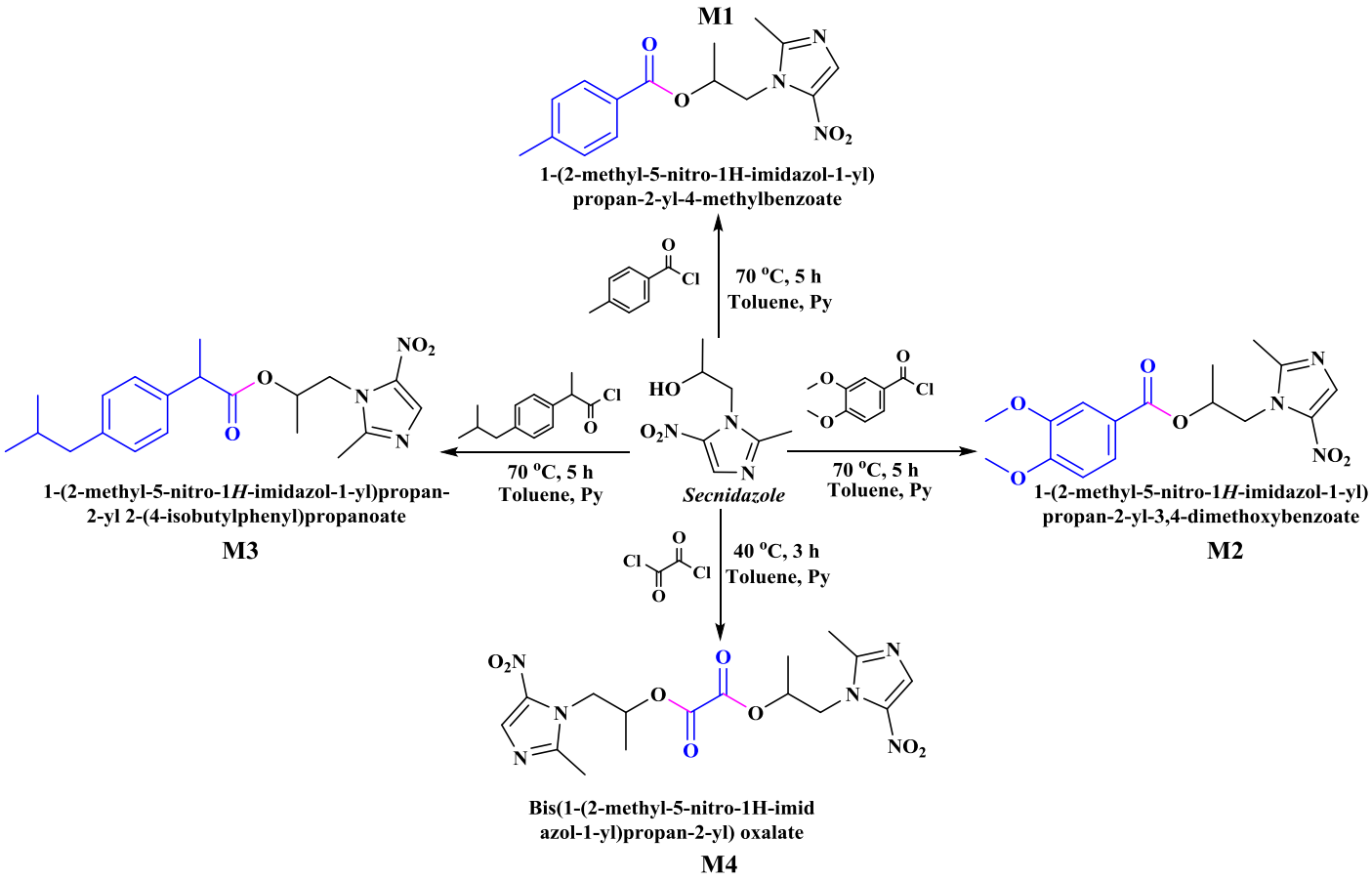

Scheme 2 Synthesis route for the Secnidazole esters (M1, M2, M3 and M4)

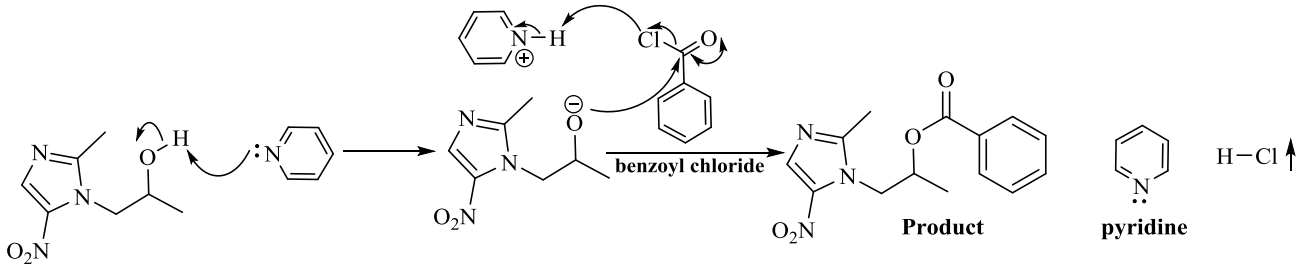

Scheme 3 Proposed esterification reaction-mechanism for the secnidazole

Scheme 4

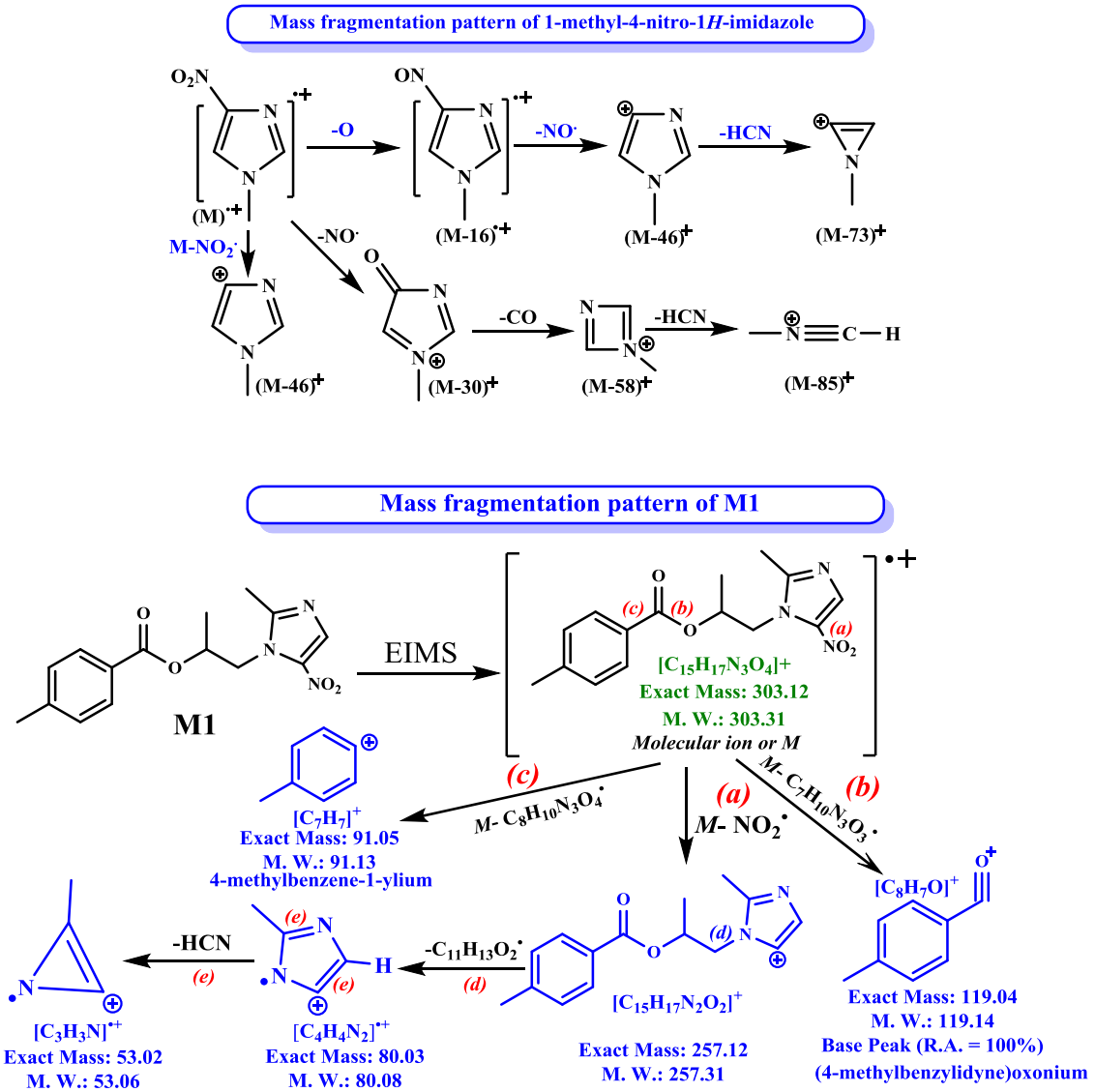
Mass fragmentation pattern of 1-methyl-4-nitro-1H-imidazole
-O
-NO·
-HCN
(M)·+
M-NO2·
-NO·
(M-16)·+
(M-46)+
(M-73)+
(M-46)+
(M-30)+
-CO
(M-58)+
-HCN
(M-85)+
Mass fragmentation pattern of M1
M1
EIMS
[C15H17N3O4]+
Exact Mass: 303.12
M. W.: 303.31
Molecular ion or M
(c)
M- C8H10N3O4·
(a)
M- NO2·
(b)
M- C7H10N3O3·
[C7H7]+
Exact Mass: 91.05
M. W.: 91.13
4-methylbenzene-1-ylium
[C8H7O]+
Exact Mass: 119.04
M. W.: 119.14
Base Peak (R.A. = 100%)
(4-methylbenzylidyne)oxonium
-C11H13O2·
(d)
[C15H17N2O2]+
Exact Mass: 257.12
M. W.: 257.31
-HCN
(e)
[C4H4N2]·+
Exact Mass: 80.03
M. W.: 80.08
[C3H3N]·+
Exact Mass: 53.02
M. W.: 53.06

Scheme 4

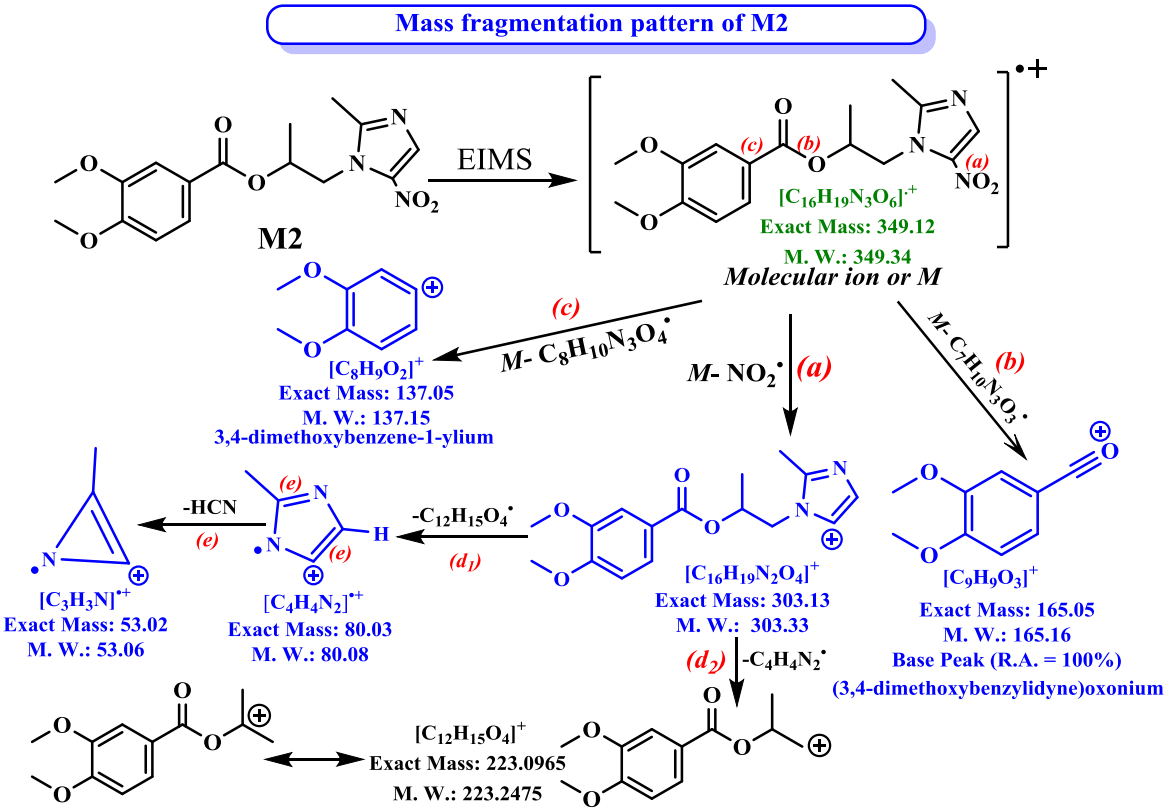
Mass fragmentation pattern of M2
M2
EIMS
[C16H19N3O6]·+
Exact Mass: 349.12
M. W.: 349.34
Molecular ion or M
(c)
M- C8H10N3O4·
[C8H9O2]+
Exact Mass: 137.05
M. W.: 137.15
3,4-dimethoxybenzene-1-ylium
M- NO2· (a)
(b)
M- C7H10N3O3·
[C16H19N2O4]+
Exact Mass: 303.13
M. W.: 303.33
-C12H15O4·
(d1)
-HCN
(e)
[C3H3N]·+
Exact Mass: 53.02
M. W.: 53.06
[C4H4N2]·+
Exact Mass: 80.03
M. W.: 80.08
[C9H9O3]+
Exact Mass: 165.05
M. W.: 165.16
Base Peak (R.A. = 100%)
(3,4-dimethoxybenzylidyne)oxonium
(d2)
-C4H4N2·
[C12H15O4]+
Exact Mass: 223.0965
M. W.: 223.2475

Scheme 4

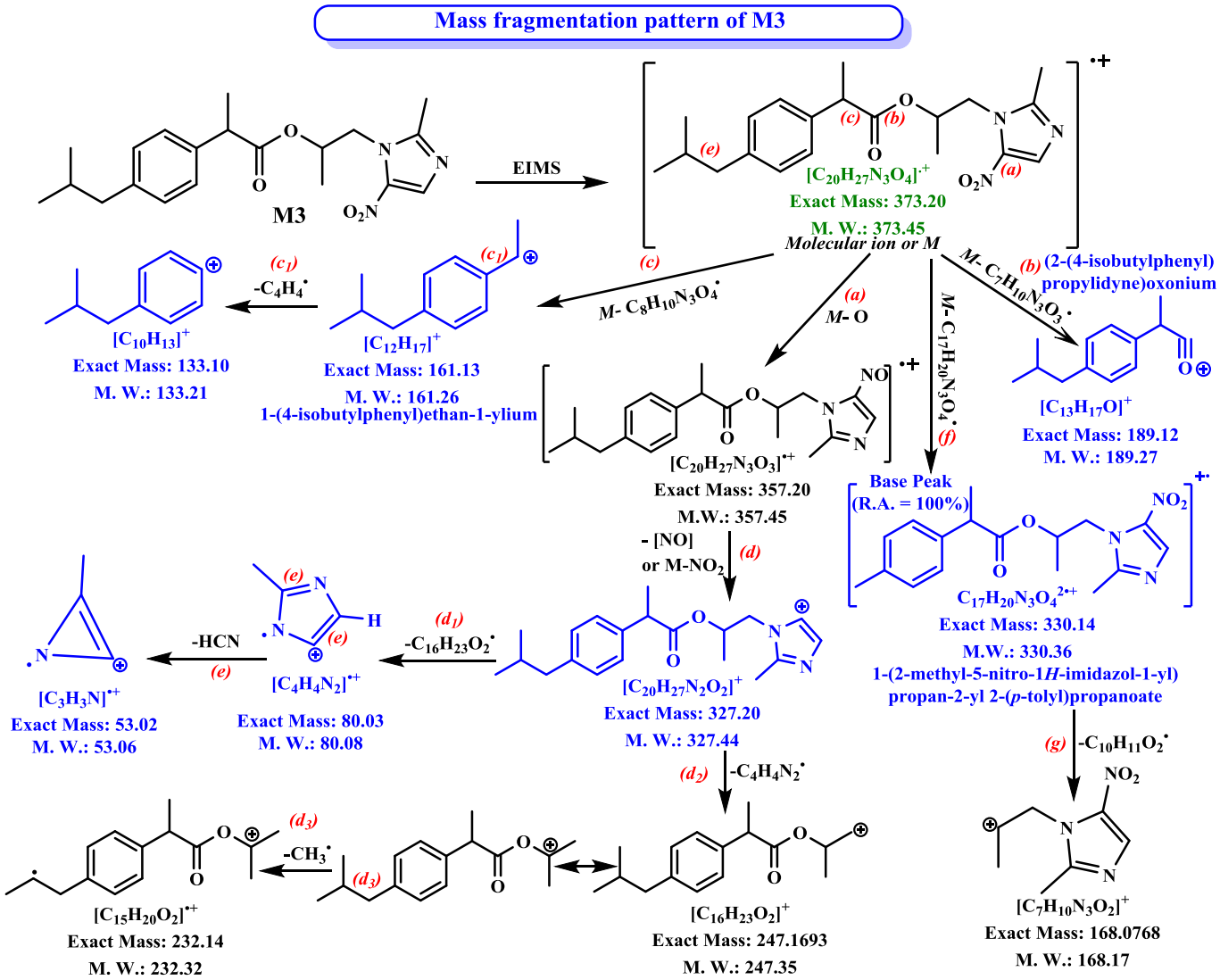
Mass fragmentation pattern of M3
M3
EIMS
[C20H27N3O4]·+
Exact Mass: 373.20
M. W.: 373.45
Molecular ion or M
(a) M- O
(b) M- C7H10N3O3·
(2-(4-isobutylphenyl) propylidyne)oxonium
(c) M- C8H10N3O4·
(c1) -C4H4·
[C10H13]+
Exact Mass: 133.10
M. W.: 133.21
[C12H17]+
Exact Mass: 161.13
M. W.: 161.26
1-(4-isobutylphenyl)ethan-1-ylium
[C13H17O]+
Exact Mass: 189.12
M. W.: 189.27
[C20H27N3O3]·+
Exact Mass: 357.20
M.W.: 357.45
(f) M-C17H20N3O4·
Base Peak
(R.A. = 100%)
C17H20N3O4 2·+
Exact Mass: 330.14
M.W.: 330.36
1-(2-methyl-5-nitro-1H-imidazol-1-yl) propan-2-yl 2-(p-tolyl)propanoate
- [NO] or M-NO2
(d) -C16H23O2·
[C20H27N2O2]+
Exact Mass: 327.20
M. W.: 327.44
(d1) -C16H23O2·
-HCN
[C4H4N2]·+
Exact Mass: 80.03
M. W.: 80.08
[C3H3N]·+
Exact Mass: 53.02
M. W.: 53.06
(d2) -C4H4N2·
(g) -C10H11O2·
[C7H10N3O2]+
Exact Mass: 168.0768
M. W.: 168.17
(d3) -CH3·
[C15H20O2]·+
Exact Mass: 232.14
M. W.: 232.32
[C16H23O2]+
Exact Mass: 247.1693
M. W.: 247.35

Scheme 4

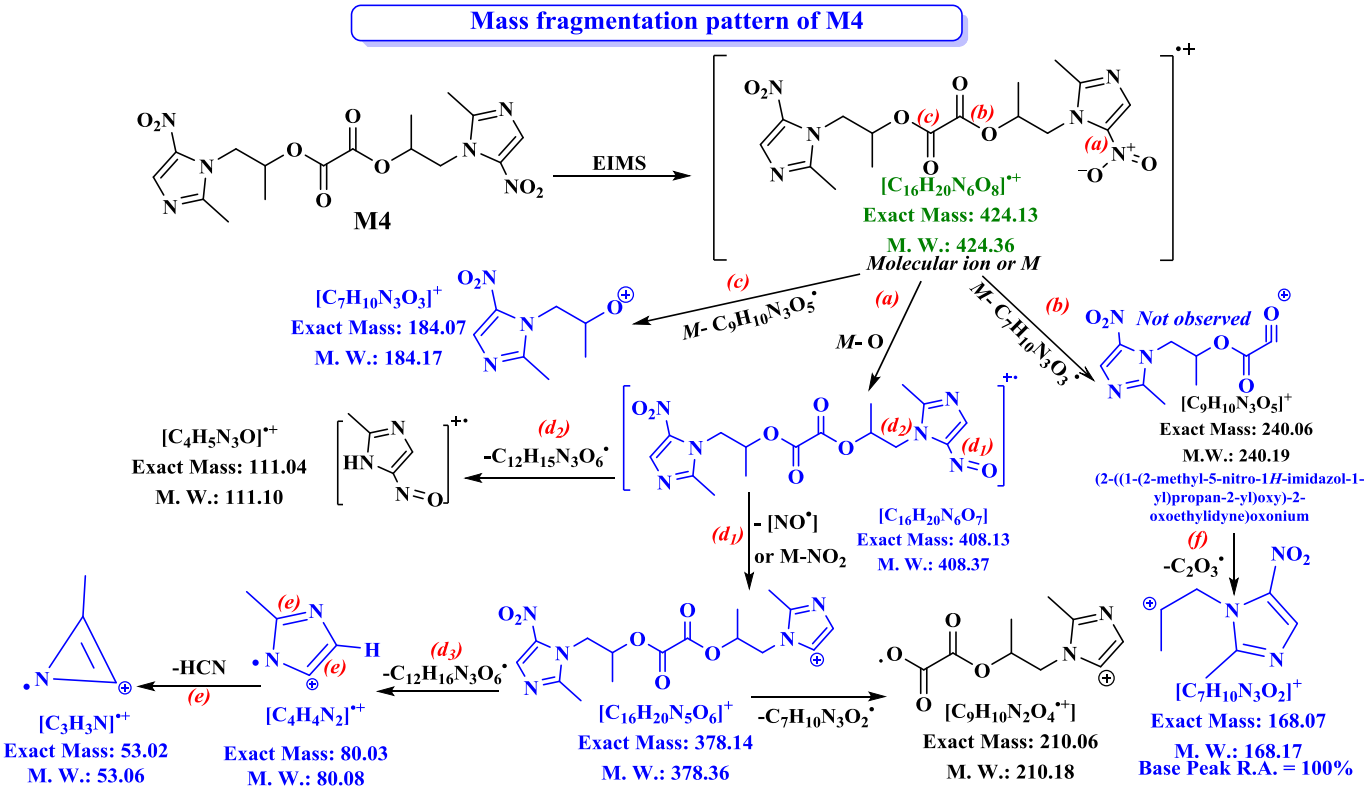
Mass fragmentation pattern of M4
M4
EIMS
[C16H20N6O8]•+
Exact Mass: 424.13
M. W.: 424.36
Molecular ion or M
(a) M- O
(b) M- C7H10N3O3•
(c) M- C9H10N3O5•
[C7H10N3O3]+
Exact Mass: 184.07
M. W.: 184.17
Not observed
[C9H10N3O5]+
Exact Mass: 240.06
M.W.: 240.19
(2-((1-(2-methyl-5-nitro-1H-imidazol-1-yl)propan-2-yl)oxy)-2-oxoethylidyne)oxonium
(f) -C2O3•
[C16H20N6O7]
Exact Mass: 408.13
M. W.: 408.37
(d1) - [NO•] or M-NO2
(d2) -C12H15N3O6•
[C4H5N3O]•+
Exact Mass: 111.04
M. W.: 111.10
[C16H20N5O6]+
Exact Mass: 378.14
M. W.: 378.36
(d3) -C12H16N3O6•
-C7H10N3O2•
[C9H10N2O4•+]
Exact Mass: 210.06
M. W.: 210.18
[C7H10N3O2]+
Exact Mass: 168.07
M. W.: 168.17
Base Peak R.A. = 100%
[C4H4N2]•+
Exact Mass: 80.03
M. W.: 80.08
-HCN (e)
[C3H3N]•+
Exact Mass: 53.02
M. W.: 53.06

Fig. 2 EIMS of M1(a), M2(b), M3(c) and M4(d).

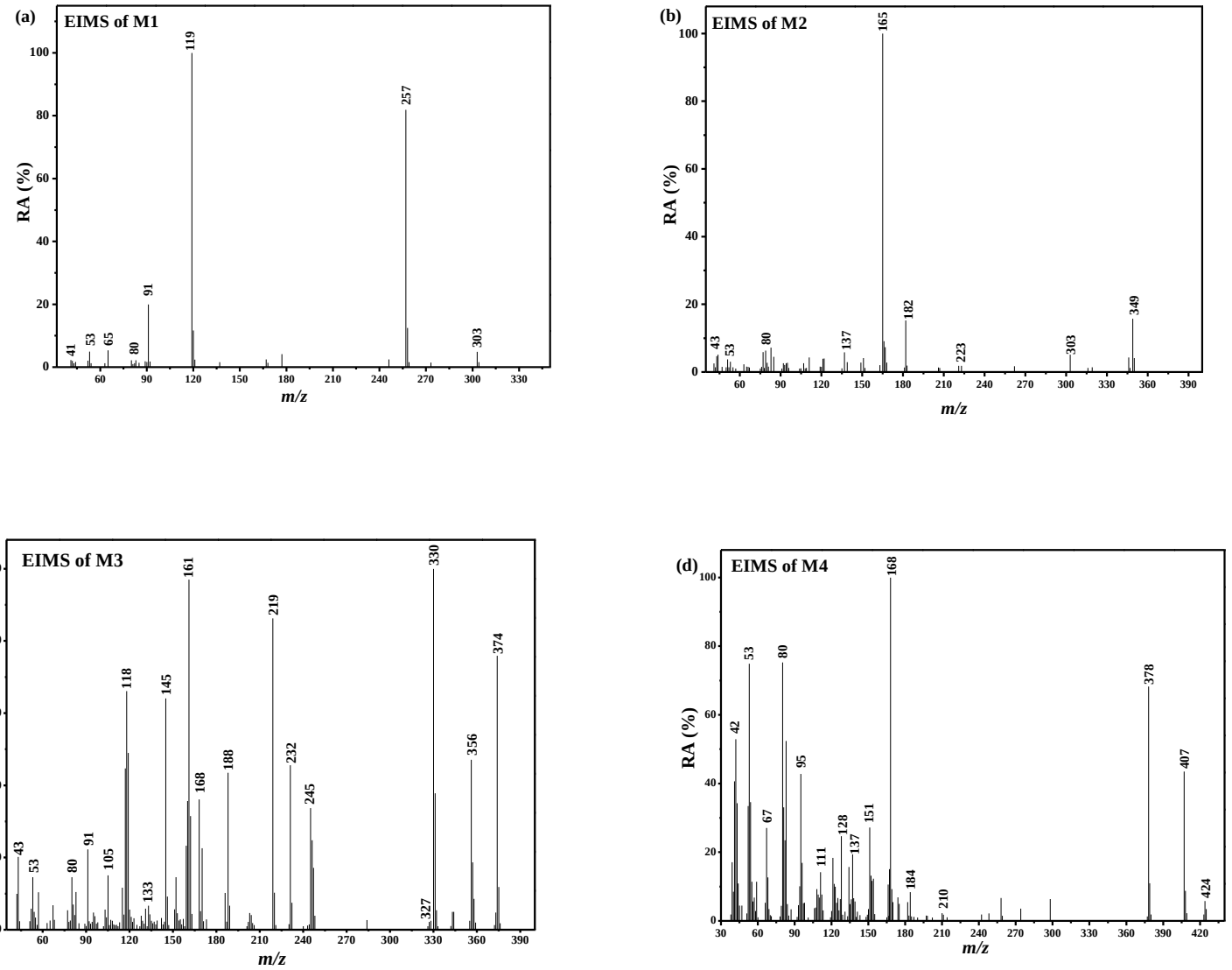

Fig. 3 FTIR of M1, M2, M3 and M4

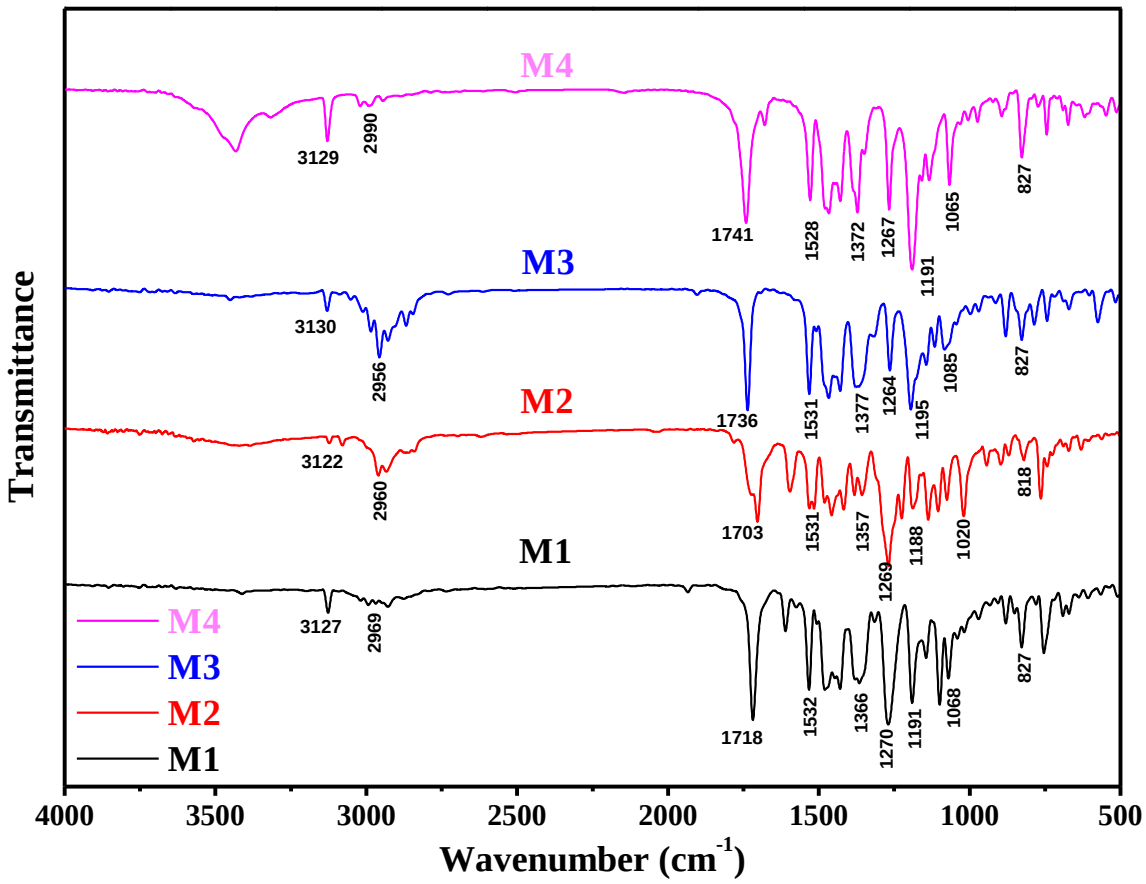

Fig. 5 UV-vis absorbance spectra (a) and Cyclic voltammograms (b) of the Secnidzole, M1, M2, M3 and M4

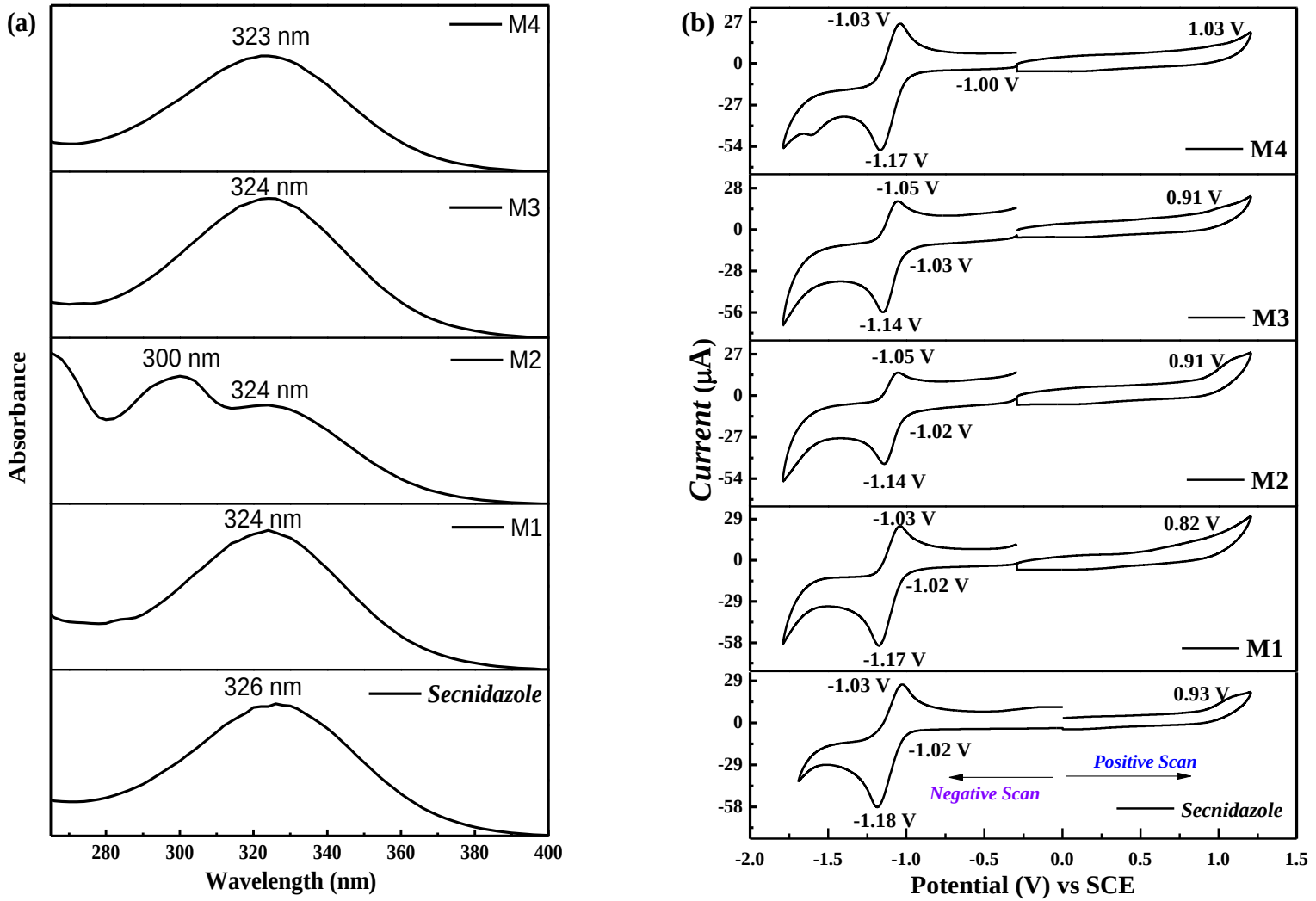

Highlights

1-A low-cost synthesis method, with less toxicity to the environment for the esterification of secnidazole is explained in detail.

2-Secnidazole esters were studied by the spectroscopic and cyclic voltammetry.

3- For secnidazole esters, ChemBioDraw Ultra 14.0 has the advantage of predicting aromatic (sp^2) carbons, while MestReNova 6.1 predicts sp^3 hybrid carbons more accurately.

4-The EIMS fragmentation analysis showed unique fragmentation patterns.